

FISSION TRACK DATING OF DETRITAL ZIRCONS
FROM THE SCOTLAND SANDSTONES,
BARBADOS, WEST INDIES

A thesis presented to the Faculty
of the State University of New York
at Albany
in partial fulfillment of the requirements
for the degree of
Master of Science

College of Science and Mathematics
Department of Geological Sciences

Suzanne Louise Baldwin

1984

FISSION TRACK DATING OF DETRITAL ZIRCONS
FROM THE SCOTLAND SANDSTONES,
BARBADOS, WEST INDIES

Abstract of
a thesis presented to the Faculty
of the State University of New York
at Albany
in partial fulfillment of the requirements
for the degree of
Master of Science

College of Science and Mathematics
Department of Geological Sciences

Suzanne Louise Baldwin

1984

ABSTRACT

Results of fission track dating of detrital zircons from the Scotland sandstones, Barbados, yield a mixture of ages with several strong groupings from 20-80 Ma, 200-350 Ma, and greater than 500 Ma. Metamict grains were assumed to fall into the greater than 500 Ma population.

The youngest population indicates that the Scotland beds, previously dated by paleontologic methods as Eocene, may actually be as young as late Oligocene. These ages better constrain the timing of deposition for these sediments and support the proposal that the late middle Eocene - early Oligocene Oceanic Fm has overthrust the Scotland beds. This population (20-80 Ma) may reflect material derived from the adjacent arc, the Netherland-Venezuelan Antilles arc, and the Caribbean Mountains of Venezuela. The 200-350 Ma population may reflect partially annealed cratonic material, an Andean component, and/or material associated with a Triassic rifting event. The oldest population (>500 Ma) and metamict zircons were very likely derived from the South American craton. $^{40}\text{Ar}/^{39}\text{Ar}$ age spectrum analysis of detrital feldspar from sample 22 provides additional evidence of a cratonic source for these sediments.

Based on results from this study, distribution of glaucophane, and paleogeographical constraints it is proposed that the source area for the Scotland sediments of Barbados was an area of the Guayana shield which was drained by the Unare (proto-Orinoco?) river system and deposited in a submarine fan north of the Unare depression.

ACKNOWLEDGEMENTS

I gratefully acknowledge the support, guidance, insight, and methodology provided to me by my advisors, Dr. Mark Harrison and Dr. Kevin Burke. Their never-ending enthusiasm and good humor has been a constant source of inspiration for me throughout this project.

This thesis benefitted from helpful discussions with Dr. Paul Mann, Dr. Steve DeLong, Daniel Loureiro, Jorge Mora, and David Bonner.

I wish to thank David Bonner, and Stephen Hutchinson for assistance in the field and the staff of Bellairs Research Institute of McGill University, Holetown, Barbados for use of their lab facilities.

I am grateful to C.W. Naeser for supervising sample irradiations at the U.S.G.S. TRIGA facility in Denver.

I wish to thank Michelle Aparisi, Karleen Davis, Kathy Stutsrim, and Bruce Idleman for technical assistance.

Support for this research was provided through DOE grant DE-AC02-82ER13013, Amoco Production Co. (International), G.S.A. grant 3107-83, and S.U.N.Y. Benevolent Fund. I would especially like to thank Sally Lewis for help in arranging support from Amoco and for assistance in the field.

Finally, a special thanks to my family, S.C.H., and Matthew for helping me keep a perspective on life during my graduate study at S.U.N.Y.

TABLE OF CONTENTS

	Page
Abstract	i
Acknowledgements	ii
List of Figures	v
List of Tables and Plates	vi
INTRODUCTION	1
Nature of the problem	1
Previous stratigraphic studies	4
CHAPTER I: GEOLOGIC SETTING	9
1.1 Introduction	9
1.2 Aves Ridge	9
1.3 Grenada Trough	9
1.4 Lesser Antilles	11
1.5 Tobago Trough	11
1.6 Barbados Ridge Complex	12
1.7 Subduction in the Lesser Antilles arc system	13
CHAPTER II: THE PRE-CORAL ROCK SECTION OF BARBADOS AS AN EXAMPLE OF AN ACCRETIONARY COMPLEX	14
2.1 Introduction	14
2.2 Sedimentation and deformation in accretionary wedges	14
2.3 Barbados as an example of an accretionary complex	18
2.4 Lithologies	19
Walkers unit	20
Morgan Lewis unit	22
Murphys unit	22
Chalky Mt. unit	25
Mt. All unit	25
2.5 Environment of deposition for Scotland beds	28
2.6 Other units cropping out on Barbados	
Joes River unit	28
Oceanic Formation	30
Bissex Hill Formation	30
Coral Rock Formation	30
CHAPTER III: FISSION TRACK DATING - SAMPLING, METHODS, AND RESULTS	33
3.1 Sampling techniques	33
3.2 Analytical techniques	33
3.3 Results	41
CHAPTER IV: PROVENANCE	55
4.1 Introduction	55
4.2 Fission track age interpretations	55
4.3 Potential source areas	
Maracaibo region of Venezuela	57
Orinoco river system	61
Unare river system	62

	Page
4.4 Distribution of glaucophane	64
4.5 Conclusion	65
CHAPTER V: ACCRETION IN THE LESSER ANTILLES ARC SYSTEM AS ILLUSTRATED BY FISSION TRACK STUDIES OF THE SCOTLAND SANDSTONES, BARBADOS	66
5.1 Introduction	66
5.2 Accretion as illustrated in the pre-coral rock section of Barbados	67
5.3 Scotland/Oceanic contact	68
5.4 Anomalous structural trend	69
5.5 Tectonic implications of fission track results	74
REFERENCES	77
APPENDIX I: THEORY AND METHODS OF FISSION TRACK DATING DATING	85

LIST OF FIGURES

Figure		Page
1.	Previously reported ages for Scotland sandstones	3
2.	Stratigraphy of Barbados; 1891-1982	7
3.	Location map of the eastern Caribbean	10
4.	Cross section of an accretionary wedge	15
5.	Accretionary processes; southern Mexico	17
6.	Photograph of Walkers unit	21
7.	Photograph of Morgan Lewis unit	23
8.	Photograph of Murphys unit	24
9.	Photograph of Chalky Mt. unit	26
10.	Photograph of Mt. All unit	27
11.	Photograph of Joes River unit	29
12.	Photograph of Oceanic Formation	31
13.-21.	Fission track results	44
22.	$^{40}\text{Ar}/^{39}\text{Ar}$ age spectrum: sample 22	53
23.	Late Paleozoic terrains of northern South America	58
24.	Geomorphological provinces of northern Venezuela and previously reported zircon fission track ages	60
25.	Distribution of active river systems in Venezuela	63
26.	Photograph of Scotland/Oceanic contact	70
27.	South American/ Caribbean plate boundary zone at end of the Oligocene	72
28.	Insert of Figure 27	73
29.	Caribbean plate boundary at approximately 28 Ma	76
30.	Track formation mechanism	86
31.	Mineral separatory techniques	92

LIST OF TABLES

Table		Page
I.	Zircon fission track data for Fish Canyon Tuff	35
II.	Zircon fission track results for Scotland sandstones	37
III.	$^{40}\text{Ar}/^{39}\text{Ar}$ age spectrum analysis for sample 22	54

PLATE 1: Generalized geology of the Scotland district and sample localities

INTRODUCTION

NATURE OF THE PROBLEM

A part of the accretionary prism of the Lesser Antilles arc system is exposed in an area of approximately 50 km² in northeastern Barbados. The rocks in this area, locally called the Scotland district, consist of semi-consolidated, deformed continental rise deposits long thought to be derived from the South American continent (Senn, 1940; Saunders, 1980). Geophysical data (Westbrook, 1982; Biju-Duval, 1982) and well-core data (Speed and Larue, 1982) indicate that these sediments may be representative of the main body of the prism.

The most detailed account of the geology of the island was written by Senn in 1940. Although we now recognize the unlikelyhood of units in an accretionary prism being stratigraphically coherent, this fact was unknown to geologists at this time. This being the case, Senn named the basal unit exposed on the island the Scotland Formation and divided it into five lithostratigraphic members. The presence of various metamorphic minerals (ie., staurolite, sillimanite, kyanite, andalusite, glaucophane, zoisite-clinozoisite, chloritoid) led Senn to suggest that the sediments were derived at least in part from a metamorphic terrane. The source of the sediments has long been debated and controversy regarding the source area has been revived with the recognition of the plate tectonic processes operating in the southern Caribbean.

The study of the rocks exposed in the Scotland District may enable us to gain insight into the processes occurring at convergent plate margins. Previous workers (Speed and Larue, 1982; Speed, 1983) have mapped the structural relationships of the rocks exposed on Barbados,

but an accurate deformation history has not been determined because of an incomplete understanding of the temporal relationships. Ages previously reported for the Scotland sediments range from early Eocene to early, late Eocene and are based on radiolarian and foraminifera preserved in the rocks (Senn, 1940; Saunders, 1979; Speed and Larue, 1982) (see Figure 1). Caudri's (1972) study emphasized the fact that much of the fauna previously dated from the Scotland rocks are worn and rolled. The fauna is heavily contaminated with reworked material from the Paleocene and many fossils were difficult to identify. If the fauna dated by paleontological methods represents re-deposited material, the ages do not provide any information concerning stratigraphic relationships. The lower Scotland beds did not contain a sufficient quantity of fossils needed for age determination by paleontological methods. Because of the lack of sufficient age control it is virtually impossible to determine an accurate deformation history for these sediments.

The present study was undertaken in order to assess the spectrum of source regions responsible for these sediments and to provide information related to the age of sedimentation. Previous petrographic studies (Senn, 1940) indicated the presence of accessory minerals suitable for fission track dating in the sandstones of the Scotland unit. Because fission track dating allows single crystals to be dated, this technique can be applied to detrital minerals to reveal their provenance age. The research described in this thesis embodies the results of fission track dating performed on detrital zircons from the Scotland sandstones of Barbados, as well as consideration of the implications of these results for the tectonic evolution of the island.

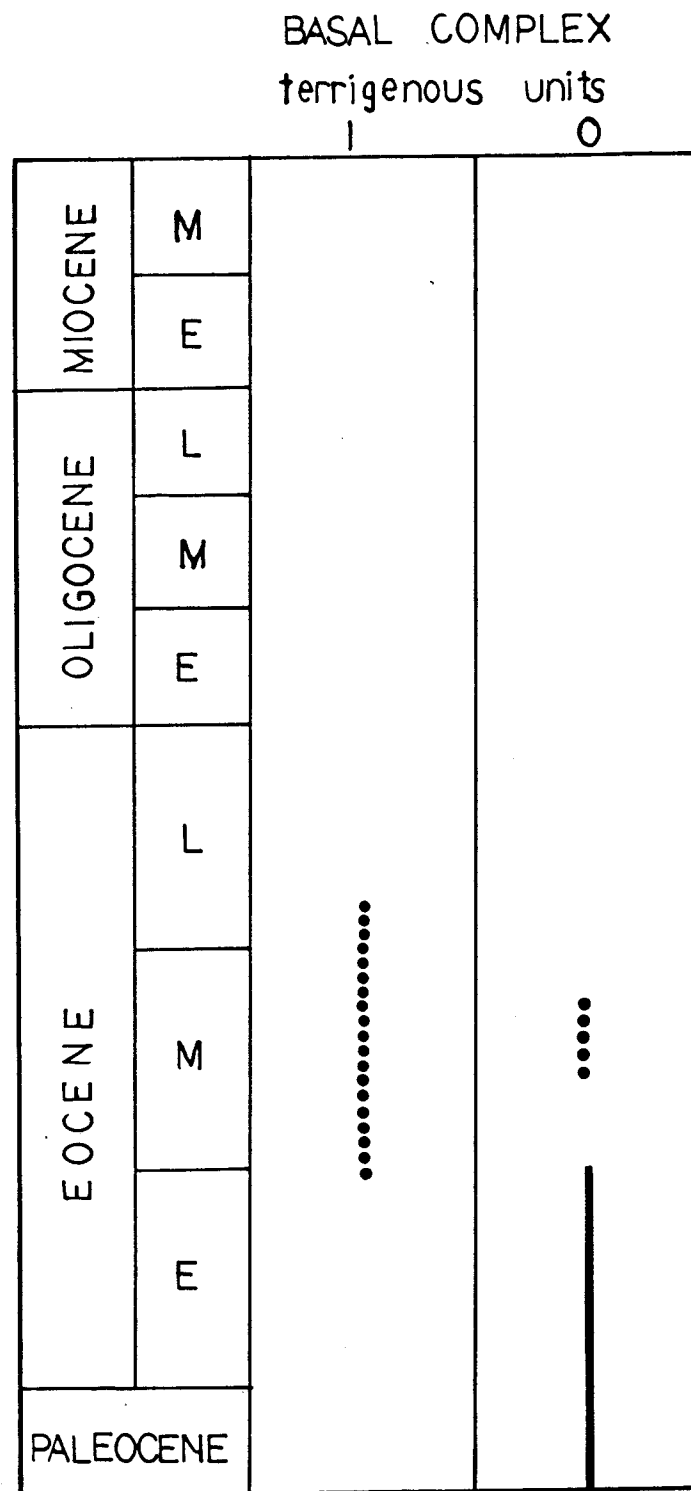


FIGURE 1:
Previously reported radiolarian ages for Scotland sandstones; solid lines indicate ranges of ages in continuous or related successions, dotted lines show allowable range of maximum ages of redeposition of some sandstones. 1= Chalky Mt. area, 0= other localities (after Speed and Larue, 1982)

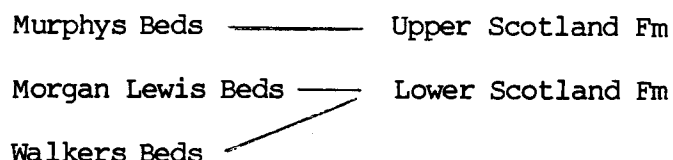
PREVIOUS STRATIGRAPHIC STUDIES

The structural complexity and the paucity of fossils dated from rocks exposed in the Scotland district have resulted in controversy concerning several aspects of these rocks. These include the environment of deposition, the age of the units, and their structure. While most workers (Saunders, 1973; Pudsey and Reading, 1982; Poole and Barker, 1983) have slightly modified Senn's nomenclature, others (Speed and Larue, 1982; Lawrence et al., 1983) have abandoned it believing that the units exposed are a pile of totally unrelated fault slices and are therefore not stratigraphically distinct units.

The first geologic map of the island was made in 1891 by Jukes-Browne and Harrison. The focus of their study was on the coral rock section which was believed to be Recent in age. The pre-coral rock section described included "Unmodified Earths and Marls", "Silicified Earths", and "Calcified Earths" (Oceanic Deposits) believed to be Pliocene. Their account did not include a description of the Scotland Beds which were believed to be pre-Miocene.

As mentioned, the most detailed and descriptive account of the islands stratigraphy was done by Alfred Senn in the late 1930's. He emphasized the pre-coral rock section and included descriptions of the Bissex Hill Fm, Globigerina Marls, Joes River Fm, and the Scotland Beds. The Scotland Beds were subdivided into five lithostratigraphic members based on the distribution of foraminifera. These members are from youngest to oldest-

Mt. All Beds ————
 Chalky Mt. Beds ———— Upper Scotland Fm



The Upper Scotland Fm was believed to be middle Eocene and the Lower Scotland Fm was lower Eocene. The Joes River Fm, lying unconformably on top of the Scotland Fm was considered to be upper Eocene. Senn also recognized blocks of Cretaceous and Paleocene limestone in the Joes River beds and Chalky Mt. member. The Oceanic Fm was believed to be upper Eocene— lower Oligocene. The Globigerina Marls were designated as late Oligocene and the coral rocks were Pleistocene. Senn was unaware that sediments in an accretionary wedge do not represent continuous stratigraphic sequences, but are tectonic units. However, his attempt to correlate the Scotland "Fm" with units in Venezuela showed great insight into the geologic processes responsible for the present position of the island.

Baadsgaard's account (1959) (in Pudsey, 1981) included descriptions of two new units - T-unit and P-unit - which were recovered from wells. Senn's Lower Scotland Fm was referred to as the River Fm and the Upper Scotland was called the Bruce Vale Fm. The Joes River Fm was not recognized as a distinct unit. Baadsgaard's Oceanic Group ranged from upper Eocene to upper Miocene and included Waterwell marls (Senn's Globigerina Marls?) and the Bissex Hill Fm. The coral rocks were assigned late Pliocene— Pleistocene ages.

Saunders (1965) noted in his field trip guide that it was difficult to distinguish between the Murphys member and the Mt. All member of the upper Scotland Fm unless they could be seen in relation to the Chalky Mt. beds. The Scotland Fm was assigned a late Paleocene—

mid - Eocene age. Saunders (1979) later suggested placing the upper and lower Scotland Fm under a generalized heading because the biostratigraphical control needed to distinguish between Senn's members does not exist.

Poole and Barker's (1983) stratigraphic column is modified from Senn (1940) and Baadsgaard (1959). They included a T-unit, which was recognized in surface exposures and boreholes, into the Upper Scotland Fm.

Pudsey and Reading's (1982) study indicates that the Scotland Fm can be correlated from block to block at outcrop. However, it is doubtful that the units occurring on different fault slices actually represent stratigraphically distinct units. A summary of the previous stratigraphic studies is shown in figure 2.

FIGURE 2: Stratigraphy of Barbados, 1891-1982, (after Pudsey, 1981)

J.R. = Joes River

	JUKES - BROWNE & HARRISON 1891	SENN 1940	BAADSGAARD 1959	SAUNDERS 1965	LOHMANN 1974	Barker & Poole 1980	Pudsey & Reading 1982
Recent	Coral Rock						
Pleistocene							
Pliocene	Oceanic deposits						
Miocene							
Oligocene	Scotland	U	Waterwell Marls	Conset Marl Fm	Oceanic Fm	Bissex Hill Fm	Oceanic Group
		M	Bissex Hill Fm	Bissex Hill Fm			
		L	Oceanic Group				
Eocene	Beds	U				J.R.	?
		M				T-unit	
		L				SCOTLAND FM	
Paleocene / Cretaceous							

Oceanic Group

Waterwell Marls
Bissex Hill Fm
T-unit
Brucevale Fm
River Fm
P-unit

Bissex Hill Fm
Globigerina Marls
Oceanic Fm
Joos River Fm
SCOTLAND FM

Scotland
Beds

U
M
L
U
M
L

Oligocene
Eocene
Paleocene /
Cretaceous

blocks

blocks

blocks

blocks

blocks

blocks

blocks

blocks

blocks

blocks

blocks

blocks

blocks

CHAPTER 1: GEOLOGIC SETTING

Introduction

The Lesser Antilles arc system is the product of the slow convergence (2-4 cm/yr) of old Atlantic seafloor (>100 Ma) with the Caribbean plate (Stein et al., 1982). The Atlantic seafloor is being subducted westward beneath the Caribbean plate and subduction occurs generally perpendicular to the arc. A thick, well-developed accretionary prism has formed in response to this convergence, and has the greatest lateral extent of any accretionary sediment pile associated with an island arc (Westbrook, 1982). From west to east, the arc system is characterized by the features described below and shown in figure 3.

Aves Ridge

The Aves Ridge forms a north-south striking topographic high extending 450 km north from the continental margin of Venezuela. It is seismically inactive. The only exposure of the ridge above sea level is Aves Island where calcareous sediments striking N70E and dipping NW and SE outcrop on the island. Dredging of the ridge has produced basalt of calc-alkaline affinities, glassy flows, volcanic breccias and granodiorites of Upper Cretaceous age (Fox and Heezen, 1971). The Aves Ridge has been interpreted as a remnant arc that was active in the Late Cretaceous (Kearey, 1974).

Grenada Trough

East of the Aves Ridge is the Grenada Trough, a feature which some have interpreted as a back arc basin (Westbrook, 1975) and others

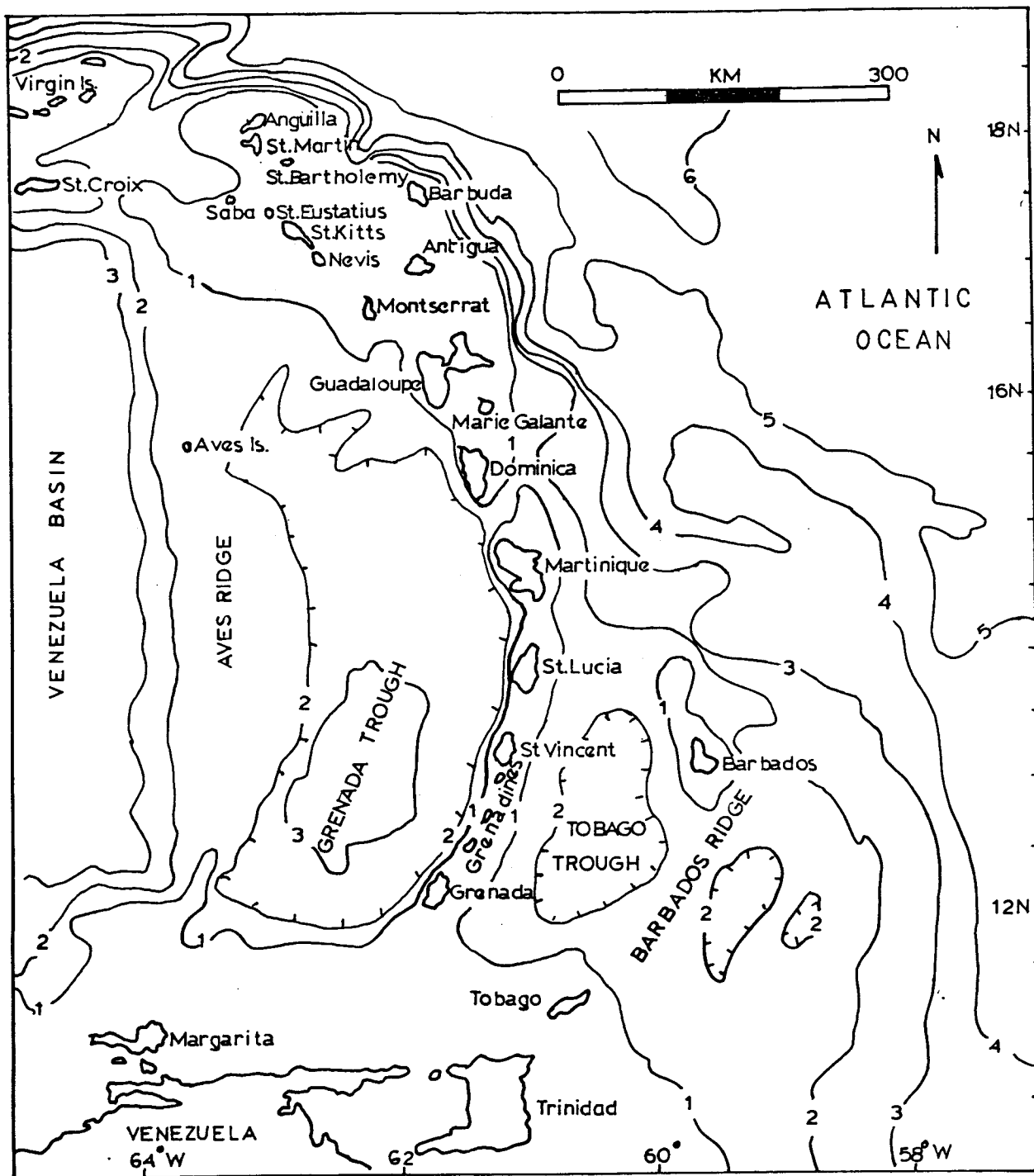


Figure 3: Location map of the eastern Caribbean. Submarine contours are in km. (Bathymetry from Westbrook, 1975.)

believe represents a piece of trapped ocean floor (K. Burke, per. comm.). Seismic data indicate the basin is filled with 4-7 km of sediments. Reflections show sediments dipping into the trough on the flanks of the basin and flat-lying sediments filling it (Westbrook, 1975).

Lesser Antilles

The volcanic chain of the Lesser Antilles forms a 700 km arc extending from Saba in the north to Grenada in the south. This topographic feature is convex towards the Atlantic and slopes steeply to the west. The arc overlies a zone of intermediate depth earthquakes (Sykes and Ewing, 1965). North of Dominica, the arc splits into an active western branch (Pliocene - Recent) and an inactive eastern branch (Oligocene). The splitting has been attributed to a reorientation of the subducting slab (Westbrook, 1975). South of Dominica, new volcanic material is inferred to have been superimposed on older volcanics. Eruptions along the arc continue today. The composition of volcanic suites vary along the arc's axis. The southern part is composed chiefly of alkaline rocks, the central part is calc-alkaline and the northern part is tholeiitic (Brown et al., 1977).

Tobago Trough

East of the southern arc lies the Tobago Trough occupying the position of a forearc basin. Seismic reflection profiles show undeformed sediments in the center of the Tobago Trough (>10 km) with deformed sediments on the flanks of the basin (Westbrook, 1975). It is bounded on the north by the Barbados- St. Lucia crosswarp and on the

south by the complex transform system associated with the South American- Caribbean plate boundary zone.

Barbados Ridge Complex

The Barbados Ridge Complex lies approximately 150 km east of the volcanic arc and consists mainly of low velocity, consolidated, deformed continental rise deposits derived from South America. This bathymetric feature is 400 km long and greater than 200 km wide. The island of Barbados marks the highest point on the ridge. In general, the bathymetry trends north-south with easterly trending ridges and troughs occurring between $13^{\circ} 30'N$ and $15^{\circ}30' N$ (Westbrook, 1975). To the south, the prism widens due to the large volume of sediment (>4 km thick) being deposited from the South American continent. There is a decrease in the thickness of the accretionary wedge northwards (to .8 km) due to the decreasing availability of sediment. This thinner sedimentary pile is more intensely deformed than its southern equivalent (Chase and Bunce, 1969). Because of the thick accumulation of sediments in the southern portion of the arc, there is no topographic expression of a trench. However, the site of the axis of a trench is indicated by a Bouguer gravity minimum (Bowin, 1976). The depth to the Benioff zone from the top of the Barbados Ridge is approximately 20 km (Westbrook, 1982). Seismic data indicate a change in seismic velocity (to 5.0 km/sec) at depths of 7 to 10 km beneath Barbados which has been interpreted to mark the presence of metamorphic rocks at this depth.

Subduction in the Lesser Antilles arc system

Seismological and magnetic evidence indicates that oceanic crust generated at the Atlantic mid-ocean ridge is moving westwards and being thrust beneath the Caribbean plate (Chase and Bunce, 1969). The zone of seismicity dips approximately 40° westwards beneath the Lesser Antilles to a depth of 200 km (Westbrook, 1975). The subduction rate has been calculated as .5 cm/yr (Chase and Bunce, 1969) or 2 cm/yr (Jordan, 1975) by different methods. Since there is no clear evidence for the location of a North American / South American / Caribbean triple junction, the subducting plate is treated as a single plate (Stein et al., 1982). The subduction zone is relatively aseismic with most of the earthquakes intraplate above the plate boundary rather than interplate on the boundary (Stein et al., 1982). The southern portion of the arc is seismically less active than the northern portion. Main shocks result from lithospheric normal faulting seaward of the trench. These faults are believed to be the result of the extension of the slab as it is subducted (Stein et al., 1982).

In summary, the southeast Caribbean plate is bounded on the east by a subduction zone and on the south by a transform fault plate boundary zone. It has been proposed that at least since 38 Ma transform motion has had a major influence on the Caribbean and South American plate boundary (Burke et al., 1978, 1984; Pindell and Dewey, 1982).

CHAPTER II: THE PRE-CORAL ROCK SECTION OF BARBADOS AS AN EXAMPLE OF AN ACCRETIONARY COMPLEX

Introduction

Accretionary wedges are complex, evolving systems where sedimentary deposition and tectonic deformation occur simultaneously. Tectonic styles vary considerably and the deformation involved is extremely complex. The older the system, the more difficult it is to reconstruct its initial configuration and to determine post- subduction deformation.

Sedimentation and Deformation in Accretionary Wedges

Structural studies of accretionary complexes have shown that the sediments within the wedge form thrust-bound packets of complex verging folds (Karig and Sharman, 1975). Sediments within the thrust packets increase in age landward. The dip of faults steepen landward and the amount of deformation also increases landward (Moore et al., 1981). Continued subduction results in a rising body of thrust slices containing chaotically mixed masses. The rising body of thrust slices provides surfaces for secondary basin formation. (see figure 4)

Tectonic style within accretionary wedges depends on the following factors:

- relationship of overriding and underriding plates
- amount and type of sediment deposited in the trench
- thickness of sediments on ocean floor
- age of crust subducted
- rate and duration of subduction

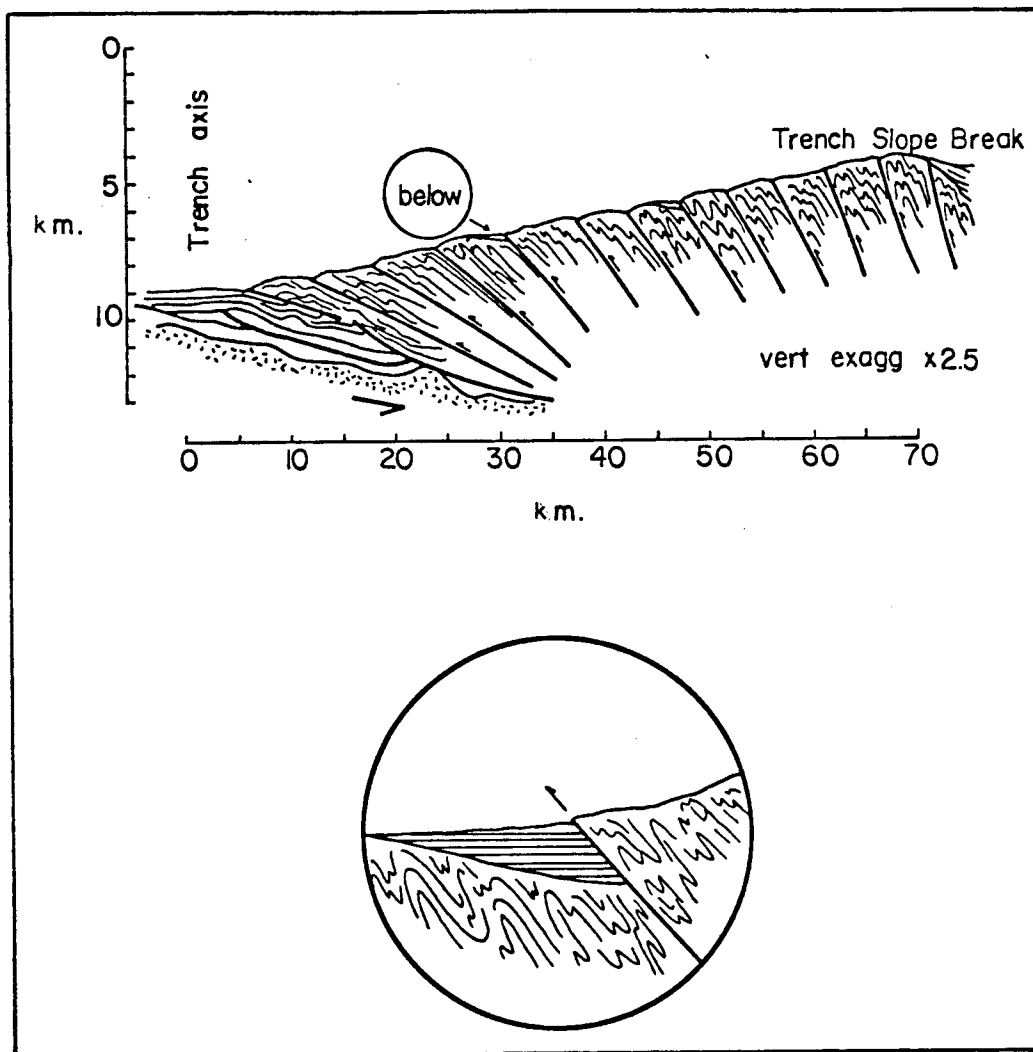


Figure 4: Accretion of thick sediment cover or thick trench-wedge section. The upper turbidite section tends to be sheared off along the weak, high-porosity uppermost pelagic section and rides over the trench wedge, probably aided by pore pressures. Insert shows secondary basin formation on rising body of thrust slices. (after Karig, 1975)

- presence of anomalous features on the descending plate
(ie., ridges, guyots, etc.)

The volume of sediment is a function not only of the amount being supplied, but also the amount of dewatering and compaction that has occurred. The relative proportions of sediment types (pelagic vs. terrigenous) is also a factor in determining the shape of the wedge. If the sediment load is large, the shallow section of the descending plate may be depressed (Westbrook, 1982).

Scholl et al. (1980) have described processes responsible for tectonic deformation of sedimentary masses at convergent margins. Subduction accretion involves the mechanical addition of material to continental or island arc margins and may cause the margin to advance oceanward. Offscraping involves the scraping off of sediments (in many cases, also oceanic crust) and the addition of this material onto the margin. Lateral tectonic accretion results from oblique subduction and involves transporting slices of material parallel to the trend of the arc. The slices are then accreted onto the margin. Underplating involves mass addition at depth beneath the accretionary wedge. (see figure 5) One would expect underplated material to be more deformed, metamorphosed, and lithologically more heterogeneous than offscraped material.

Sediment subduction involves transporting sediments on the downgoing plate beneath the crystalline basement of the underthrust margin. Horst and graben features on the downgoing plate may cause larger volumes of sediment to be subducted. Subduction erosion occurs when the margin is thinned as a result of its interaction with the descending plate. Extensive subduction erosion may cause landward

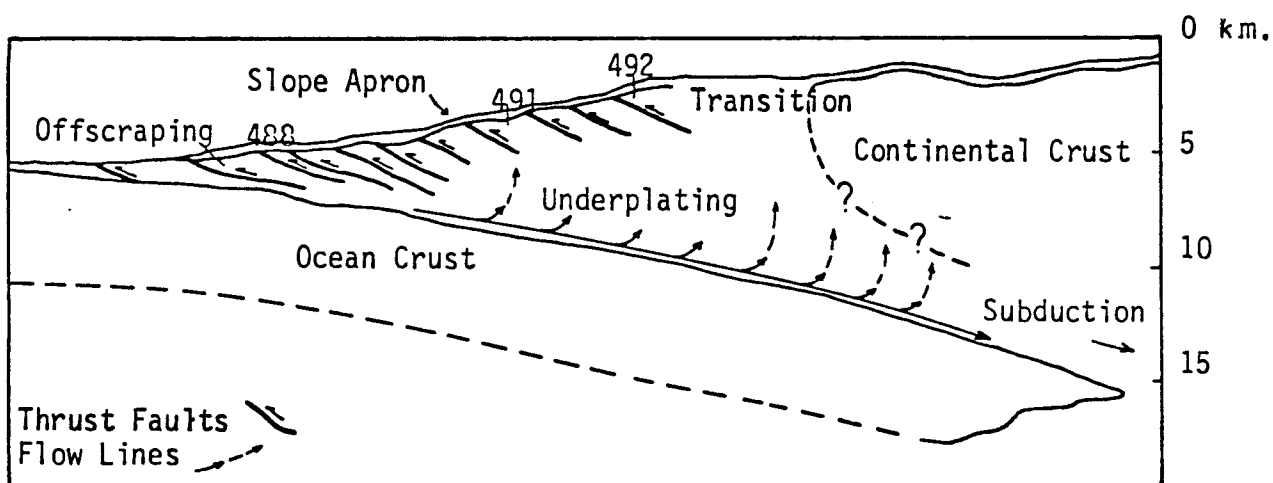


Figure 5: Accretionary processes responsible for shape of accretionary terrane, southern Mexico. Composite structural section based on seismic data and drilling results. Offscraped trench deposits constitute external rind of accretionary terrane beneath which underplating occurs. Solid arrows in underplating zone describe particle flow for a short time interval. Dashed arrows represent long-term particle motion due to growth of the accretionary prism over geologic time. Mass balance calculations indicate sediment subduction. (after Moore et al., 1981)

retreat of the inner trench wall resulting in exposure of older material. Where the underriding and overriding plates are strongly coupled, accretion and tectonic erosion may be competing processes.

Barbados as an Example of an Accretionary Complex

There are very few places in the world where sediments within active accretionary wedges can be directly observed (ie. Nias, Nicobar Islands, Kodiak, Barbados). The accretionary wedge associated with the Lesser Antilles arc system is wider in its southern portion due to the high sediment feed rate from the South American continent. The amount of sediment deposited directly in the trench in front of the arc and the amount that was deposited on the ocean floor is unknown. The basal complex of Barbados is believed to be an exposed portion of the main prism body associated with the Lesser Antilles arc system. Field observations and regional geophysical data indicate that continuous deformation and uplift of accreted sediments and deposition of hemipelagic sediments have been the dominant processes involved in the formation of Barbados (Speed, 1983; Westbrook, 1982.)

The structure of the accretionary complex exposed at Chalky Mt. consists of six fault-bounded packets which strike E-NE and have steep dips. Fault boundaries have been interpreted to be surfaces of accretion (Speed, 1983). Older hemipelagic rocks and turbidites are highly deformed but the younger hemipelagic rocks are less disrupted. The rocks are not metamorphosed implying that there has been little, if any, advective circulation within the prism (Speed, 1983). However, Westbrook (1982) has recorded seismic velocities of 5.0 km/sec at depths of 7-10 km which he interprets to be metamorphic rocks. The

presence of unmetamorphosed sediments implies that they represent offscraped and not underplated deposits. Quaternary reefs record rapid and differential uplift from .6-.7 Ma (Mesolella et al., 1969). The uplift may be due to local diapirism (mud diapirs of the Joes River unit) or to vertical transport of accreted material (Speed, 1983).

Steeply dipping fault bounded packets in the crestal zones of accretionary wedges are also found in the Aleutian arc and Sunda arc. However, folding is a more dominant feature in Barbados than in those cited above. In accretionary wedges where rates of subduction are low and large volumes of sediment are present, folding seems to be the dominant structural feature. In environments with low volumes of sediment and moderately high subduction rates , the dominant mechanism is shearing and disruption of strata (Karig, 1980).

Lithologies

Six-sevenths of the land surface of Barbados is covered by Quaternary coral reef limestones. An eroded half dome in the northeastern part of Barbados exposes older Tertiary units. These crop out in a series of east-northeast trending fault bounded blocks (see plate 1). Senn (1940) divided the basal unit of Barbados into five lithostratigraphic members comprising the Lower and Upper Scotland Fm. In general, the rocks consist of graywackes and mudstones. Because of complex repetition of the Scotland beds, the total thickness has not been accurately determined and may mean little.

The following is a description of the various units exposed on the island of Barbados.

Walkers Unit

The type section for this unit is located northeast of the Bawden and Rivers Estate (Senn, 1940). Excellent exposures can be examined along the ridge where overturned beds dip steeply (70° NW) and strike N60E. At this location the following sequence can be observed. Ironstone bands (5-6 cm thick) containing flattened dark blue and gray shale pebbles (2-3 cm thick and 6-10 cm in diameter) are common with flute casts on the underside. These are overlain by approximately 2 m of laminated green and light gray clayey siltstones. Micaceous, light gray and tan, massively-bedded sandstone (.2-.8 m) overlies the siltstones. The base of the sandstone bed is sharp, ironstained, and contains flute and groove casts indicating current direction was from the southwest. Abundant sedimentary features characteristic of turbidite sequences are present. These include graded bedding, dish and pillar structures, and slump features. On top of the sandstones lie approximately .3 m of thickly laminated, micaceous, ferruginous, foliated clayey siltstone and tan-light gray sandy siltstone which weathers to a yellow color. Green-brown clays overlain by 7-8 cm of cone-on-cone limestone form the top of the sequence. The sequence is repeated across the ridge. Cone-on-cone limestone and ironstone bands form the most resistant beds. The sandstone to shale for this unit is approximately 40:60. Senn (1940) measured the thickness of this unit at the type locality (240 m), although wells drilled indicate thicknesses may exceed more than 650 m. At this locality the unit is isoclinally folded and overturned.

Morgan Lewis Unit



Figure 6: Walkers unit showing tan, massively bedded sandstone with graded bedding and dish and pillar structures. Green clays overlie sandstone. Locality is north of Bawden and Rivers Estate.

The outcrops examined are located on the ridge northeast of Morgan Lewis Windmill and south of Choyce, along the coast. The section northeast of the windmill consists almost entirely of claystone shale striking N50E and dipping 50° NW with beds overturned. Alternating layers of green-blue-gray clay-rich shale and white clay with lenses of calcareous, light, medium-brown claystone shale are also present. Ironstone bands (6 cm) thick with flute and groove casts on the sole surface grade into stained calcareous grit at this locality. Thinly-laminated, light tan, silty clays contain dish structures and convolute bedding. The ratio of sandstone to shale at this locality is approximately 20:80. Gypsum crystals (2-3 cm) are common on bedding planes. Light tan, massively-bedded, fine-grained sandy claystone was sampled south of Choyce.

Murphys unit

This unit consists entirely of clay and siltstone striking N75E and dipping 55° SE. Good exposures are located near Spa House and west of Barclays Park. The bulk of the section contains thinly laminated carbonaceous brown-purple clays and pale yellow-tan clays with ironstained tops and thinly laminated white, light gray siltstone. Fluid escape features and slump folds are common. No consistent paleoslope was obtained from the slump folds (Pudsey, 1981). Gypsum (.5-1 cm) crystals are present on clay bedding surfaces. Minor amounts of fine-grained, tan, yellow, micaceous siltstone with calcareous cement is present as well. These contain ripple cross laminations and vertical burrows. It is difficult to distinguish these beds from the Mt. All unit unless they can be seen above or below the Chalky Mt. unit



Figure 7: Morgan Lewis unit (sample 29) showing faulted micaceous, light tan, fine-grained sandstone. Locality is south of Choyce along the coast.

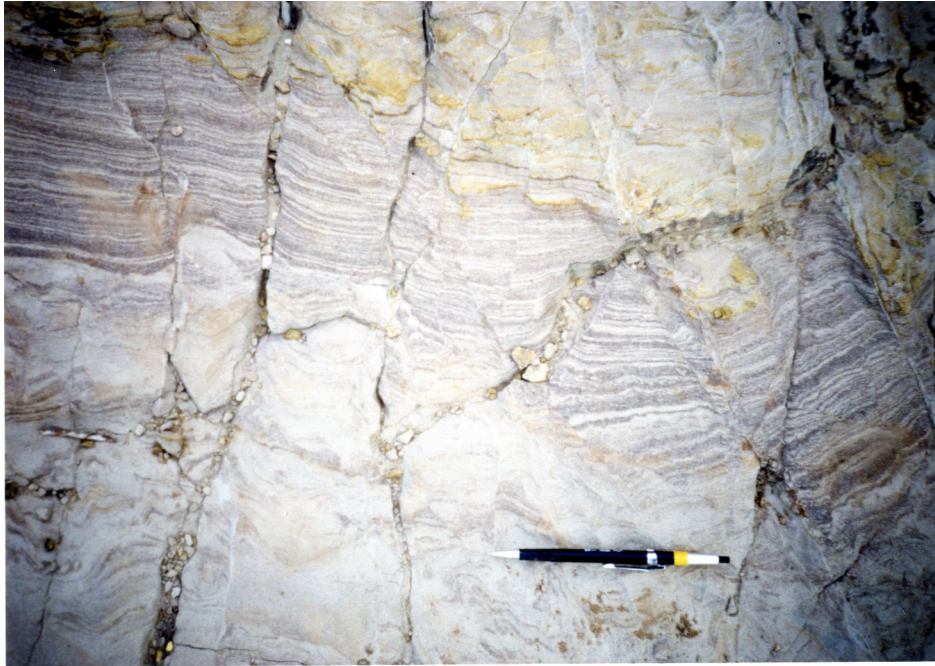


Figure 8: Murphys unit showing highly faulted, thinly laminated purple and tan clays. Locality is near Spa House.

at outcrop.

Chalky Mt. Unit

The type section is located at Chalky Mt. where excellent exposures are found at the base and at the summit. This unit also caps the Morgan Lewis clays at Greenland and outcrops in the quarry east of Springfield. The Chalky Mt. unit consists mainly of massive, white, friable, coarsegrained sandstones and are the coarsest sandstones within the Scotland district. Quartz grains are subangular to subrounded and are generally clear, although milky and blue quartz can be seen in grits outcropping at the summit. The matrix is non-calcareous and clayey. Lenses of cross-bedded, green, silty clays occur and nodules of light, gray-purple clays occasionally occur within the sands. At the base of Chalky Mt. graded sandstone (5 m thick) are ironstained at the base and contain flattened pebbles. Measurements of the total thickness for this unit vary between 90-200 m (Senn, 1940).

Mt. All Unit

The Mt. All unit is characterized by complex, steeply plunging features. Excellent outcrops of this unit can be examined at Mt. All and Map Hill located north of Springfield. This member consists mainly of alternating light tan-white, massive, friable, medium-coarse grained sandstone and reddish brown, thinly laminated silty clays. The sandstones are graded, ironstained at the base, and cross bedding can be seen at the top of the sandstone layers. Sand predominates with a sandstone to shale ratio of 90:10. Sulfur occurs on the bedding planes of clays.



Figure 9: Chalky Mt. unit showing massively bedded, white, coarse grained, friable grits in clayey matrix. Lenses of cross-bedded green clays are present in the sandstone. Locality is base of Chalky Mt. along the East Coast Road.



Figure 10: Mt. All unit showing contorted anticline consisting of alternating graded sandstone and laminated light purple siltstone. Locality: Mt. All.

Environment of Deposition For Scotland Beds

The depositional environment for the Scotland beds has been a topic of debate for almost a century (Jukes-Browne and Harrison, 1891; Senn, 1940; Pudsey and Reading, 1982; Speed and Larue, 1982; Poole and Barker, 1983). Abundant sedimentary features characteristic of turbidites have led most authors to suggest that these sediments were deposited by turbidity currents in a deep marine environment. Pudsey and Reading (1982) determined that possible environments of deposition for these sediments are:

- by mass flow processes in a deep sea trench
- in a submarine fan fed by a submarine canyon
- in an abyssal cone fed by a broad delta.

Other Units Cropping Out On Barbados

Joes River Unit

The Joes River formation has not been accurately dated and has been described as a melange "sensu lato" (Pudsey and Reading, 1982). It consists of dark gray-black, foliated organic mudstone with angular inclusions of green clay. It contains a variety of allochthonous blocks consisting of radiolarians, sand inclusions, and limestone. The limestone blocks are Paleocene (Senn, 1940; Caudri, 1972). The origin of this formation is not known although the most accepted interpretation is that the mudstones are a product of sedimentary volcanism. This interpretation is supported by the facts that the contacts are often sharp and fault-like, the mudstones are often found in the cores of anticlines, and large xenoliths of country rock are



Figure 11: Allochthonous hemipelagic block in Joes River unit located south of Map Hill.

common around the margins (Poole and Barker, 1983). The Joes River unit bears a strong resemblance to hydrocarbon rich mud volcanoes on the south coast of Trinidad (Senn, 1940; Pudsey and Reading, 1982).

Oceanic Formation

Excellent exposures of the Oceanic rocks can be observed at Cluffs Bay, Gays Cove, and Bathsheba. The Oceanic unit consists of deep water pelagic foraminiferal and radiolarian marls ranging from late middle Eocene to early Oligocene (Saunders, et al., 1984). Volcanic ash, presumably derived from the adjacent arc is present in the bottom half of the unit. Maximum thickness is 450 m, and paleobathymetric studies indicate that these sediments were deposited at depths of 1000-5000 m (Saunders, 1979). The Oceanic rocks lie on top of the Scotland beds, but the nature of this contact has been a subject of controversy (Speed and Larue, 1982; Pudsey and Reading, 1982). An unconformity exists between the Oceanic unit and the overlying units.

Bissex Hill Formation

This unit crops out in a small area on top of Bissex Hill and consists of lower Miocene yellow foraminiferal limestone and loose sand. Paleodepths were between 300-1500 m at the time of deposition (Saunders, 1979).

Coral Rock Formation

Quaternary coral limestone reef terraces cover the land area surrounding the Scotland district. The best exposures can be found on the east coast. Outcrops of reef terraces can be found inland as well,



Figure 12: Oceanic unit showing white chalk and radiolarian earths with interbedded ash layers. Locality: Bath cliffs.

but these tend to be located in inaccessible areas due to dense foliation. Results from stratigraphic studies and radioactive dating indicate that the limestone terraces are uplifted coral reefs that were deposited during periods of relatively high sea level (Bender et al., 1979). Additional Quaternary deposits include dune deposits, river alluvium, and terrace deposits.

CHAPTER III: FISSION TRACK DATING - SAMPLING, METHODS, AND RESULTS

Sampling Techniques

Eight samples of coarse-grained sandstone were collected for this study from the Scotland district of Barbados. Four of the units of the Scotland group and a Pleistocene sand dune deposit were sampled. Approximately 16 liters of material was collected from surface outcrops at each locality (see Plate 1). The coarsest material was sampled with the expectation that they would contain sufficiently large zircons for dating by the fission track technique. Although all of the samples were friable and weathered, previous work has shown that weathering has no effect on track stability/retention in zircons (Gleadow and Lovering, 1975).

Analytical Techniques

The techniques used in the preparation and dating of zircons by the fission track method are described in detail by Naeser (1973), Gleadow and Lovering (1975) and Harrison (1977). The external detector method of fission track dating was used for all analyses and is described in Appendix I. Initial mineral separations were conducted at Bellairs Research Institute of McGill University, Holetown, Barbados, and consisted of eluting the samples in seawater and panning the clean sands for a heavy mineral concentrate. Final mineral separation involving heavy liquid and magnetic techniques was performed at the Department of Geological Sciences, SUNY at Albany.

Zircons were recovered in sufficient quantities for analysis from the concentrate for all samples collected. However, apatite was exceedingly scarce, and no concentrates were obtained. Muscovite

detectors were used as the external detectors to record the induced track density. Samples were irradiated in the USGS TRIGA reactor in Denver, Colorado, under the supervision of C.W. Naeser. NBS standard glasses 962 with mica external detectors were used as neutron dosimeters (Carpenter and Reimer, 1974). Zircon standards from the Fish Canyon Tuff provided by C.W. Naeser were used as an internal check on the calibrations of glass standards. Using the accepted age of Fish Canyon, 27.5 ± 1.3 Ma (1 σ) (Naeser, 1981), the calculated flux fell within uncertainty of that determined using the glass standards. Fission track analytical data for Fish Canyon Tuff are presented in Table 1.

All fission track counting was done using an oil immersion lens at 1250 x magnification. A geometry factor of 0.5 was assumed for the external detector method (Gleadow and Lovering, 1977). Dates were calculated using the fission track equation:

$$\text{Age} = \frac{1}{\lambda_D} \ln \left[1 + \left(\frac{\rho_s}{\rho_i} \cdot \frac{\lambda_D \Phi \sigma I}{\lambda_F} \right) \right],$$

where λ_D and λ_F are ^{238}U decay constants for alpha emission and spontaneous fission respectively, Φ is the thermal neutron dose, I is the atomic ratio of uranium isotopes $^{235}\text{U}/^{238}\text{U}$ and σ is the cross section for neutron fission reaction of ^{235}U and ρ_s and ρ_i are spontaneous and induced track densities, respectively. Substituting numerical constants into the above equation gives the working form of the fission track age equation.

$$t = 6.446 \times 10^9 \ln \left[1 + (0.5) \frac{\rho_s}{\rho_i} \Phi (9.283 \times 10^{-18}) \right] \text{ years}$$

The constants used in the calculation of ages are listed in Table 1. Ages produced using the above equation represent the time elapsed since

TABLE I
FISSION TRACK DATA AND AGES FOR ZIRCONS FROM
FISH CANYON TUFF AGE STANDARD

Sample No.	$\rho_s \text{ cm}^{-2}$	$\rho_i \text{ cm}^{-2}$	ϕ $\times 10^{15} \text{ neutrons/cm}^2$	Age Ma (± 1)
Grain 1	4.94×10^5 (171)	4.48×10^5 (155)	1.06	34.0 ± 3.8 Ma
Grain 2	5.32×10^5 (184)	6.13×10^5 (212)	1.06	27.5 ± 2.8 Ma
Grain 3	6.85×10^5 (237)	7.25×10^5 (251)	1.06	29.9 ± 2.7 Ma
Grain 4	6.65×10^5 (230)	7.05×10^5 (244)	1.06	29.8 ± 2.8 Ma
Total	2.37×10^6 (822)	2.49×10^6 (862)		30.2 ± 1.6 Ma

NOTE:

ρ_s = spontaneous track density; ρ_i = induced track density; ϕ = neutron dose

$\lambda_f = 7.03 \times 10^{-17} \text{ yr}^{-1}$, $^{235}\text{U}/^{238}\text{U} = 7.252 \times 10^{-3}$, $\sigma^{235} = 580.2 \times 10^{-24} \text{ cm}^2$, $\lambda_d = 1.551 \times 10^{-10} \text{ yr}^{-1}$

Numbers in parentheses are tracks counted to determine the reported track density.

the mineral cooled to a temperature enabling track retention. The closure temperature for zircons is approximately 200°C over periods of geologic time (Gleadow, 1975). Previous work (Larue et al., 1983; S. Lewis, per. comm.) based on organic thermal indicators determined that these sediments have experienced maximum temperatures of 75°C which is insufficient to anneal fission tracks in zircons. Analytical results are presented in Table 2. Uncertainties in the ages shown were calculated using standard statistical methods. In this study, each sample was numbered so that it could be counted without knowing its identity.

Binocular observations of the concentrates indicated that a bimodal distribution of zircons exists in all samples; clear, euhedral grains and rounded, pink, variably radiation damaged grains. Previous petrographic studies (Pudsey and Reading, 1982) showed a similar bimodal distribution of quartz grains from the Scotland sands, consisting of 1/3 large, clear, unstrained quartz grains and 2/3 strained, polycrystalline quartz grains; the latter presumably plutonic or metamorphic in origin.

Based on the characteristics of the zircon grains, the samples were split and each split etched for two different durations. The two mounts made for each sample were etched for approximately 10 hours and 2 hours in order to resolve tracks in the "young" and "old" zircons, respectively. Details of this procedure are described in Appendix I. This approach insured that the total countable zircon population could be measured. The effect of this etching bias is unclear as sample mounts yielded a broad range of ages. (see Table 2). Only the mount of sample 28 that was etched for 2 hours did not reveal fission tracks

TABLE II
FISSION TRACK RESULTS

Sample Number	$\rho_s \text{ cm}^{-2}$	$\rho_i \text{ cm}^{-2}$	Φ $\times 10^{15} \text{ neutrons/cm}^2$	Age Ma $\pm 1\sigma$
38A	9.36×10^5 (324)	4.02×10^5 (139)	1.03 ($\pm 1.7\%$)	71.0 ± 7.0
38A	1.09×10^6 (189)	1.62×10^5 (28)	1.03 ($\pm 1.7\%$)	204.0 ± 42.0
38A	4.10×10^5 (142)	2.20×10^5 (76)	1.03 ($\pm 1.7\%$)	57.0 ± 8.0
38A	1.71×10^6 (296)	2.25×10^5 (39)	1.03 ($\pm 1.7\%$)	229.0 ± 39.0
38A	1.82×10^6 (315)	1.56×10^5 (27)	1.03 ($\pm 1.7\%$)	349.0 ± 60.0
38B	5.75×10^5 (199)	6.01×10^5 (208)	1.04 ($\pm 1.7\%$)	30.0 ± 3.0
38B	7.35×10^5 (61)	1.08×10^6 (90)	1.04 ($\pm 1.7\%$)	21.0 ± 3.5
38B	3.33×10^6 (288)	2.08×10^5 (18)	1.04 ($\pm 1.7\%$)	480.0 ± 120.0
38B	5.26×10^5 (91)	7.46×10^5 (129)	1.04 ($\pm 1.7\%$)	22.0 ± 3.0
38B	7.54×10^5 (73)	8.98×10^5 (87)	1.04 ($\pm 1.7\%$)	26.0 ± 4.0
38B	2.37×10^6 (460)	3.82×10^5 (74)	1.04 ($\pm 1.7\%$)	190.0 ± 24.0
38A	6.50×10^5 (90)	9.39×10^4 (13)	1.03 ($\pm 1.7\%$)	210.0 ± 62.0
29A	9.75×10^5 (54)	4.15×10^5 (23)	1.04 ($\pm 1.7\%$)	73.0 ± 18.0
29A	5.66×10^5 (49)	4.5×10^5 (39)	1.04 ($\pm 1.7\%$)	39.0 ± 8.4
29A	1.31×10^6 (295)	6.67×10^4 (15)	1.04 ($\pm 1.7\%$)	586.0 ± 150.0
29A	2.08×10^6 (115)	1.43×10^6 (79)	1.04 ($\pm 1.7\%$)	45.0 ± 6.6
29A	2.98×10^6 (515)	1.45×10^5 (25)	1.04 ($\pm 1.7\%$)	612.0 ± 126.0
29A	1.34×10^6 (74)	4.87×10^5 (27)	1.04 ($\pm 1.7\%$)	85.0 ± 19.0
29B	9.30×10^5 (161)	6.94×10^5 (120)	1.06 ($\pm 1.7\%$)	42.0 ± 5.0
29B	1.62×10^6 (157)	7.12×10^5 (69)	1.06 ($\pm 1.7\%$)	72.0 ± 10.0
29B	3.76×10^6 (208)	8.13×10^5 (45)	1.06 ($\pm 1.7\%$)	145.0 ± 24.0
29B	1.08×10^6 (105)	4.02×10^5 (39)	1.06 ($\pm 1.7\%$)	85.0 ± 16.0

TABLE II (continued)

Sample Number	$\rho_s \text{ cm}^{-2}$	$\rho_i \text{ cm}^{-2}$	ϕ $\times 10^{15} \text{ neutrons/cm}^2$	Age Ma $\pm 1\sigma$
29B	1.76×10^6 (292)	1.99×10^5 (33)	1.06 ($\pm 1.7\%$)	274.0 ± 54.0
35A	3.99×10^6 (152)	3.42×10^5 (13)	1.03 ($\pm 1.7\%$)	352.0 ± 102.0
35A	4.31×10^6 (179)	3.13×10^5 (13)	1.03 ($\pm 1.7\%$)	360.0 ± 97.0
35A	5.32×10^6 (221)	3.61×10^5 (15)	1.03 ($\pm 1.7\%$)	800.0 ± 290.0
35A	2.53×10^5 (14)	1.45×10^5 (8)	1.03 ($\pm 1.7\%$)	29.0 ± 11.0
35A	5.26×10^5 (91)	8.67×10^4 (15)	1.03 ($\pm 1.7\%$)	87.0 ± 18.0
35A	4.34×10^5 (30)	4.62×10^5 (32)	1.03 ($\pm 1.7\%$)	51.0 ± 15.0
35B	2.44×10^6 (135)	3.25×10^5 (18)	1.05 ($\pm 1.7\%$)	345.0 ± 104.0
35B	3.18×10^6 (176)	2.17×10^5 (12)	1.05 ($\pm 1.7\%$)	247.0 ± 56.0
35B	1.66×10^6 (144)	2.54×10^5 (22)	1.05 ($\pm 1.7\%$)	172.0 ± 37.0
35B	2.14×10^6 (148)	3.76×10^5 (26)	1.05 ($\pm 1.7\%$)	376.0 ± 113.0
35B	2.02×10^6 (140)	1.73×10^5 (12)	1.05 ($\pm 1.7\%$)	357.0 ± 107.0
35B	2.63×10^6 (91)	3.47×10^5 (12)	1.05 ($\pm 1.7\%$)	157.0 ± 41.0
28A	3.00×10^5 (52)	1.97×10^5 (34)	1.08 ($\pm 1.7\%$)	49.0 ± 11.0
28A	1.97×10^6 (239)	2.40×10^5 (29)	1.08 ($\pm 1.7\%$)	262.0 ± 52.0
28A	1.79×10^6 (309)	1.10×10^5 (19)	1.08 ($\pm 1.7\%$)	507.0 ± 120.0
28A	2.80×10^6 (242)	1.62×10^5 (14)	1.08 ($\pm 1.7\%$)	537.0 ± 148.0
28A	1.88×10^6 (130)	2.75×10^5 (19)	1.08 ($\pm 1.7\%$)	218.0 ± 54.0
28A	1.55×10^6 (107)	5.78×10^4 (4)	1.08 ($\pm 1.7\%$)	813.0 ± 414.0
22A	2.50×10^6 (433)	2.14×10^5 (37)	1.09 ($\pm 1.7\%$)	373.0 ± 64.0
22A	1.65×10^6 (229)	4.12×10^5 (57)	1.09 ($\pm 1.7\%$)	130.0 ± 20.0
22A	3.21×10^6 (278)	1.97×10^5 (17)	1.09 ($\pm 1.7\%$)	515.0 ± 129.0
22A	3.41×10^6 (118)	2.02×10^5 (7)	1.09 ($\pm 1.7\%$)	530.0 ± 207.0

TABLE II (continued)

Sample Number	$\rho_s \text{ cm}^{-2}$	$\rho_i \text{ cm}^{-2}$	ϕ $\times 10^{15} \text{ neutrons/cm}^2$	Age Ma $\pm 1\sigma$
22A	2.14×10^5 (37)	2.83×10^5 (49)	1.09 ($\pm 1.7\%$)	25.0 ± 5.0
22A	3.95×10^5 (86)	3.17×10^5 (69)	1.09 ($\pm 1.7\%$)	41.0 ± 7.0
22B	3.20×10^6 (277)	1.27×10^5 (11)	1.08 ($\pm 1.7\%$)	766.0 ± 236.0
22B	2.14×10^6 (370)	6.36×10^4 (11)	1.08 ($\pm 1.7\%$)	$1,000.0 \pm 300.0$
22B	4.86×10^5 (84)	2.77×10^5 (48)	1.08 ($\pm 1.7\%$)	56.0 ± 10.0
22B	2.86×10^6 (247)	4.39×10^5 (38)	1.08 ($\pm 1.7\%$)	207.0 ± 36.0
22B	2.20×10^6 (183)	5.66×10^5 (47)	1.08 ($\pm 1.7\%$)	125.0 ± 21.0
22B	2.12×10^6 (147)	2.17×10^5 (15)	1.08 ($\pm 1.7\%$)	309.0 ± 84.0
27A	1.55×10^6 (537)	2.69×10^5 (93)	1.09 ($\pm 1.7\%$)	185.0 ± 21.0
27A	2.24×10^6 (774)	9.25×10^4 (32)	1.09 ($\pm 1.7\%$)	742.0 ± 135.0
27A	1.65×10^6 (143)	2.77×10^5 (24)	1.09 ($\pm 1.7\%$)	191.0 ± 42.0
27A	1.41×10^6 (122)	4.62×10^5 (40)	1.09 ($\pm 1.7\%$)	98.0 ± 18.0
27A	1.32×10^6 (458)	5.52×10^5 (191)	1.09 ($\pm 1.7\%$)	78.0 ± 7.0
27A	5.40×10^5 (187)	2.05×10^5 (71)	1.09 ($\pm 1.7\%$)	85.0 ± 12.0
27B	2.76×10^6 (239)	3.70×10^5 (32)	1.07 ($\pm 1.7\%$)	235.0 ± 44.0
27B	3.95×10^6 (342)	1.70×10^6 (147)	1.07 ($\pm 1.7\%$)	74.0 ± 7.0
27B	3.91×10^6 (338)	4.62×10^5 (40)	1.07 ($\pm 1.7\%$)	265.0 ± 45.0
27B	4.16×10^6 (288)	5.20×10^5 (36)	1.07 ($\pm 1.7\%$)	251.0 ± 45.0
26A	2.49×10^5 (43)	2.43×10^5 (42)	1.09 ($\pm 1.7\%$)	33.0 ± 7.0
26A	2.09×10^5 (58)	9.75×10^4 (27)	1.09 ($\pm 1.7\%$)	70.0 ± 16.0
26A	9.02×10^5 (156)	4.80×10^5 (83)	1.09 ($\pm 1.7\%$)	61.0 ± 8.0
26A	7.80×10^5 (135)	8.21×10^5 (142)	1.09 ($\pm 1.7\%$)	31.0 ± 4.0
26A	1.03×10^6 (89)	7.63×10^5 (66)	1.09 ($\pm 1.7\%$)	44.0 ± 7.0
26A	1.90×10^6 (329)	8.67×10^4 (15)	1.09 ($\pm 1.7\%$)	680.0 ± 180.0

TABLE II (continued)

Sample Number	$\rho_s \text{ cm}^{-2}$	$\rho_i \text{ cm}^{-2}$	ϕ $\times 10^{15} \text{ neutrons/cm}^2$	Age Ma $\pm 1\sigma$
26B	1.34×10^6 (93)	1.59×10^5 (11)	1.08 ($\pm 1.7\%$)	266.0 ± 85.0
26B	5.78×10^5 (60)	3.37×10^5 (35)	1.08 ($\pm 1.7\%$)	55.0 ± 12.0
26B	2.15×10^6 (186)	2.43×10^5 (21)	1.08 ($\pm 1.7\%$)	280.0 ± 64.0
26B	1.62×10^6 (112)	1.45×10^5 (10)	1.08 ($\pm 1.7\%$)	350.0 ± 116.0
26B	2.50×10^5 (13)	1.93×10^5 (10)	1.08 ($\pm 1.7\%$)	42.0 ± 18.0
26B	7.23×10^5 (125)	7.17×10^5 (124)	1.08 ($\pm 1.7\%$)	32.0 ± 4.0
26A	2.89×10^5 (80)	8.44×10^5 (73)	1.09 ($\pm 1.7\%$)	36.0 ± 6.0
30A	1.44×10^6 (499)	7.80×10^4 (27)	1.04 ($\pm 1.7\%$)	550.0 ± 110.0
30A	4.77×10^5 (99)	2.94×10^5 (61)	1.04 ($\pm 1.7\%$)	50.0 ± 8.0
30A	3.21×10^6 (278)	1.85×10^5 (16)	1.04 ($\pm 1.7\%$)	518.0 ± 133.0
30A	9.53×10^4 (33)	1.07×10^5 (37)	1.04 ($\pm 1.7\%$)	28.0 ± 7.0
30A	2.73×10^6 (170)	7.06×10^5 (44)	1.04 ($\pm 1.7\%$)	119.0 ± 20.0
30A	7.88×10^5 (109)	1.95×10^5 (27)	1.04 ($\pm 1.7\%$)	124.0 ± 27.0
30B	1.65×10^6 (143)	2.89×10^5 (15)	1.05 ($\pm 1.7\%$)	294.0 ± 80.0
30B	2.09×10^6 (116)	5.78×10^5 (32)	1.05 ($\pm 1.7\%$)	113.0 ± 23.0
30B	3.29×10^6 (228)	7.23×10^5 (50)	1.05 ($\pm 1.7\%$)	142.0 ± 22.0
30B	1.50×10^6 (260)	2.43×10^5 (42)	1.05 ($\pm 1.7\%$)	192.0 ± 32.0
30B	1.98×10^6 (171)	2.20×10^5 (19)	1.05 ($\pm 1.7\%$)	278.0 ± 67.0
30B	1.61×10^6 (139)	2.66×10^5 (23)	1.05 ($\pm 1.7\%$)	188.0 ± 42.0
30A	3.76×10^5 (130)	1.10×10^5 (38)	1.04 ($\pm 1.7\%$)	105.0 ± 20.0

NOTE: "A" samples etched for 10 hrs.
 "B" samples etched for 2 hrs.
 For sample localities, see Plate 1.

suitable for counting.

RESULTS

Results yield a mixture of ages with several strong groupings from 20-80 Ma, 200-350 Ma, and greater than 500 Ma (Table II, Fig. 13-21). Metamict grains in each sample that disintegrated during etching were assumed to fall into the greater than 500 Ma group as the induced track density was not indicative of sufficiently high uranium concentrations to cause younger zircons to become metamict. Analytical data and metamict grains counted are combined and shown in histograms (see Figures 13-21).

Sample 38, (Fig. 21) collected from the Walkers unit yielded the youngest ages clustering around 25 Ma. It is likely that grains etched for 2 hrs. from this sample were underetched, and as a result, the ages can be regarded as "too" young. Results from this sample were strikingly similar to those from sample 26, collected from the Mount All unit. However, grains etched for 2 hrs. and 10 hrs. from sample 26 gave similar ages. In general, the youngest population in all samples ranged from 20 - 90 Ma with strong groupings clustering around 30 Ma. These ages indicate that the Scotland rocks, previously dated by paleontological methods as Eocene, may actually be as young as late Oligocene. These are the youngest ages reported for these rocks, and probably reflect contributions from Lesser Antilles ash falls, reworked sediments of the accretionary prism, and sediments derived from the Netherland Antilles and Coastal Complex of Northern Venezuela. These potential source areas are described in detail in Chapter IV. Ages from this population (>25 Ma) better constrain the timing of deposition

for these sediments and also supports the suggestion that the late middle Eocene - early Oligocene Oceanic Formation has overthrust the Scotland rocks (see Chapter V). Youngest ages, from grains etched for 10 hrs., provide at best a maximum age of deposition, but the extent to which these sediments have been reworked remains unknown. Large variations are found from unit to unit within the Scotland rocks and within the same unit further indicating that the Scotland rocks do not form a continuous stratigraphic succession as discussed in Chapter II.

Additional populations show strong groupings between 200 - 350 Ma and greater than 500 Ma. A gap exists for all samples between 350 - 480 Ma. While it is not clear what source area the 200 - 350 Ma grains represent, they were probably derived from uplifted areas in northern South America. Grains with ages greater than 500 Ma reflect material derived from the South American craton. Sample 22, collected from the Chalky Mount unit yielded the oldest fission tracks age found in this study of 1 Ga. $^{40}\text{Ar}/^{39}\text{Ar}$ age spectrum analysis of K-feldspar separated from this sample yield what is interpreted to be a slow cooling gradient (Harrison and McDougall, 1982) between 1350 - 925 Ma (see Table 3 and Figure 22).

Sample 30, collected from a late Pleistocene (?) sand dune (Poole and Barker, 1983) gave a mixture of ages with a strong concentration of ages at 100 - 200 Ma.






In summary, fission track dating of detrital zircons from the Scotland sandstones indicates that these rocks may be significantly younger (late Oligocene) than previously determined (Eocene). Youngest ages give an estimate of the time of deposition for these sediments although the extent to which they have been reworked is unknown. Older

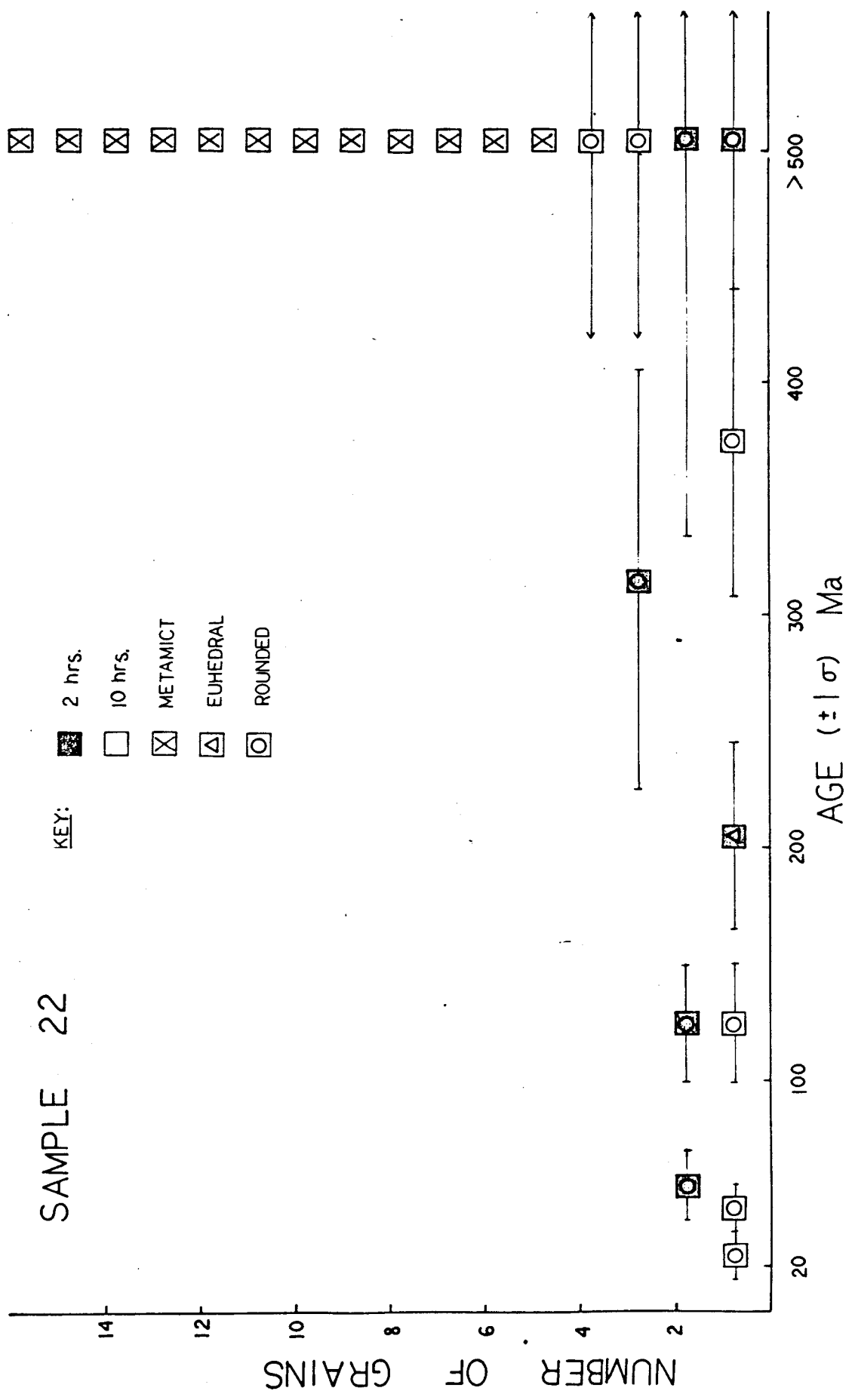
populations provide information pertaining to the source area for these rocks and indicate a substantial contribution was derived from the South American craton (see Chapter IV).

FIGURES 13-21: Results of fission track dating on detrital zircons from the Scotland sandstones, Barbados. See plate 1 for sample localities.

SAMPLE 22



KEY:




-  2 hrs.
-  10 hrs.
-  METAMICT
-  EUHEDRAL
-  ROUNDED

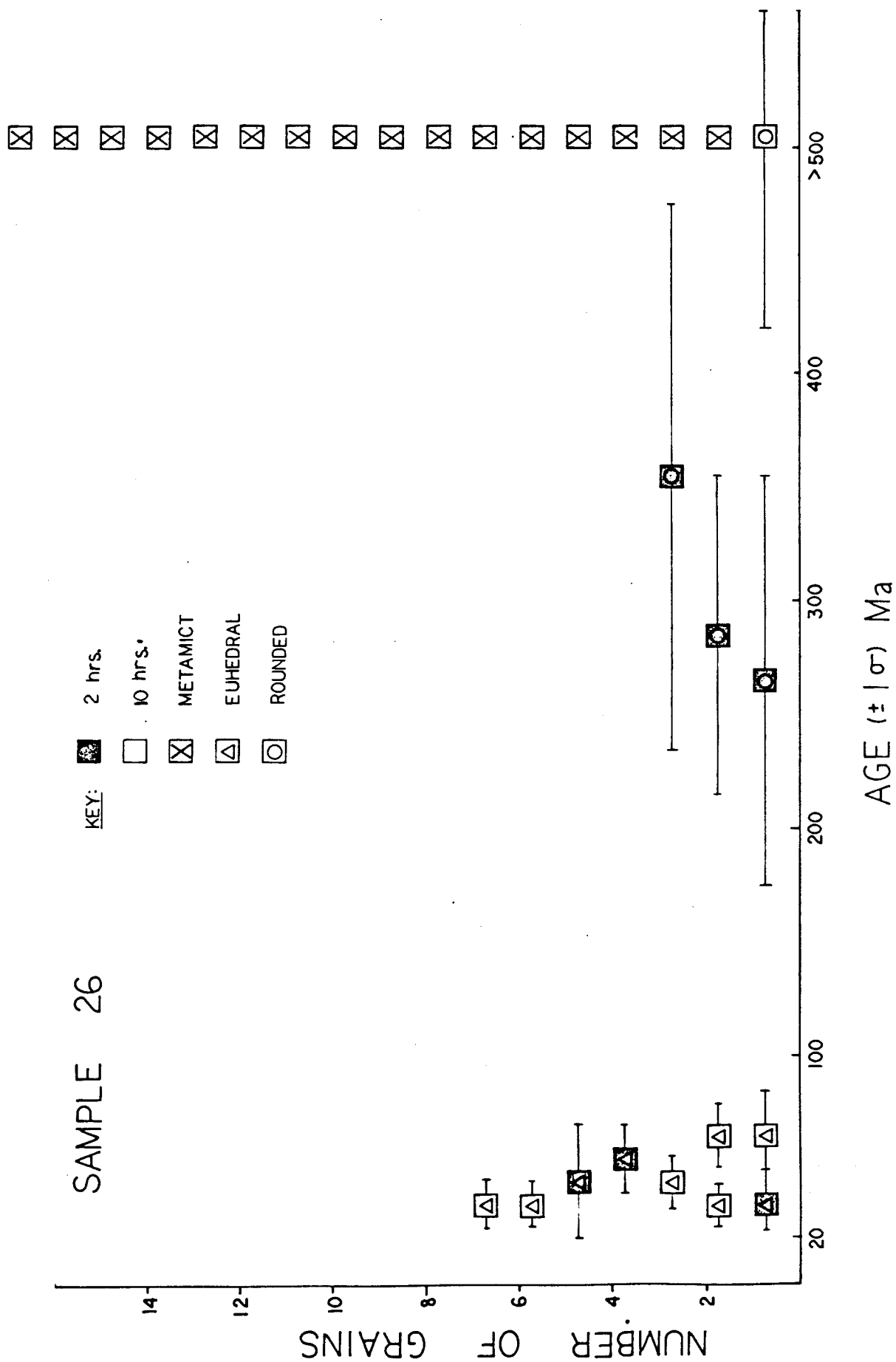


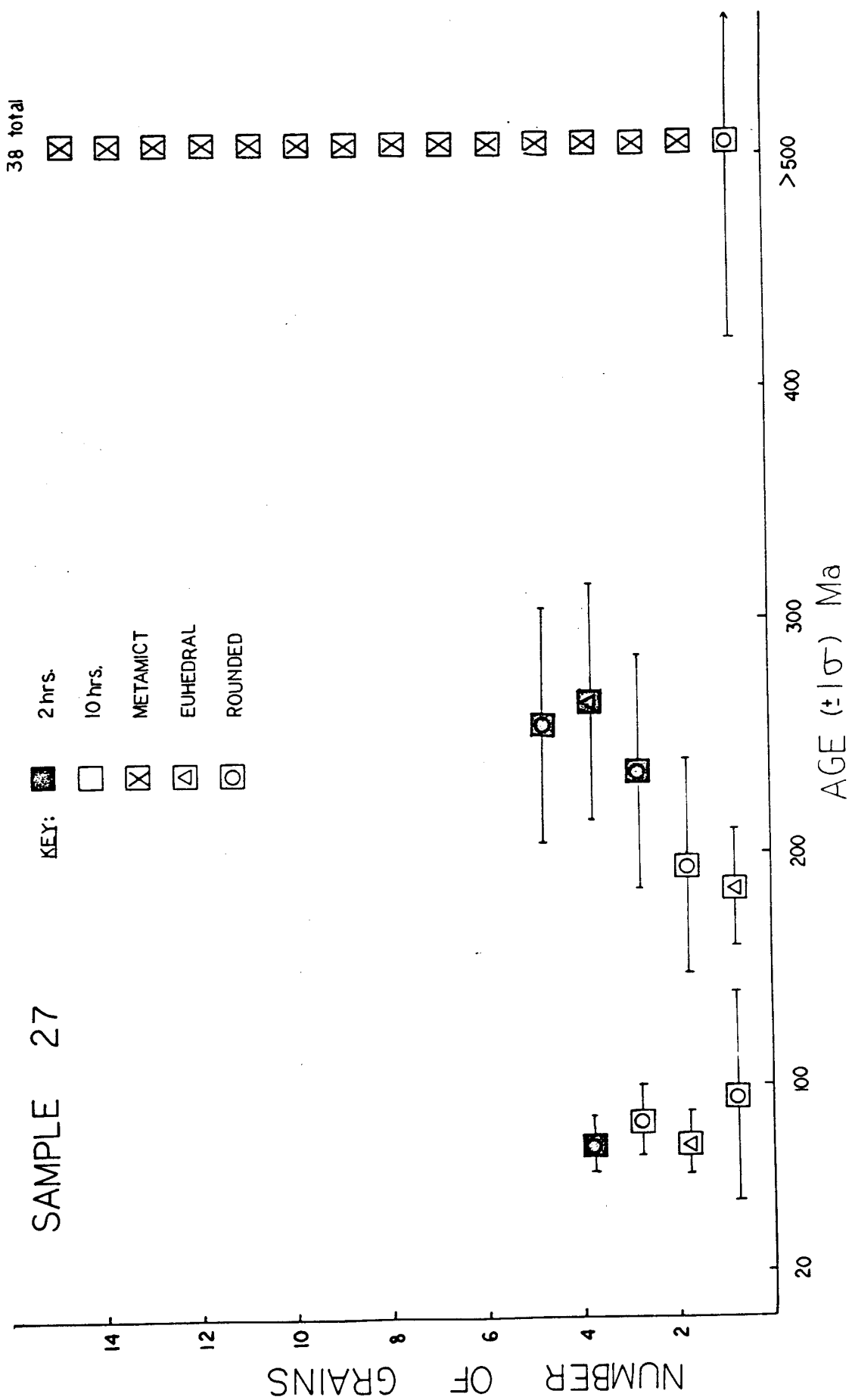
SAMPLE 26

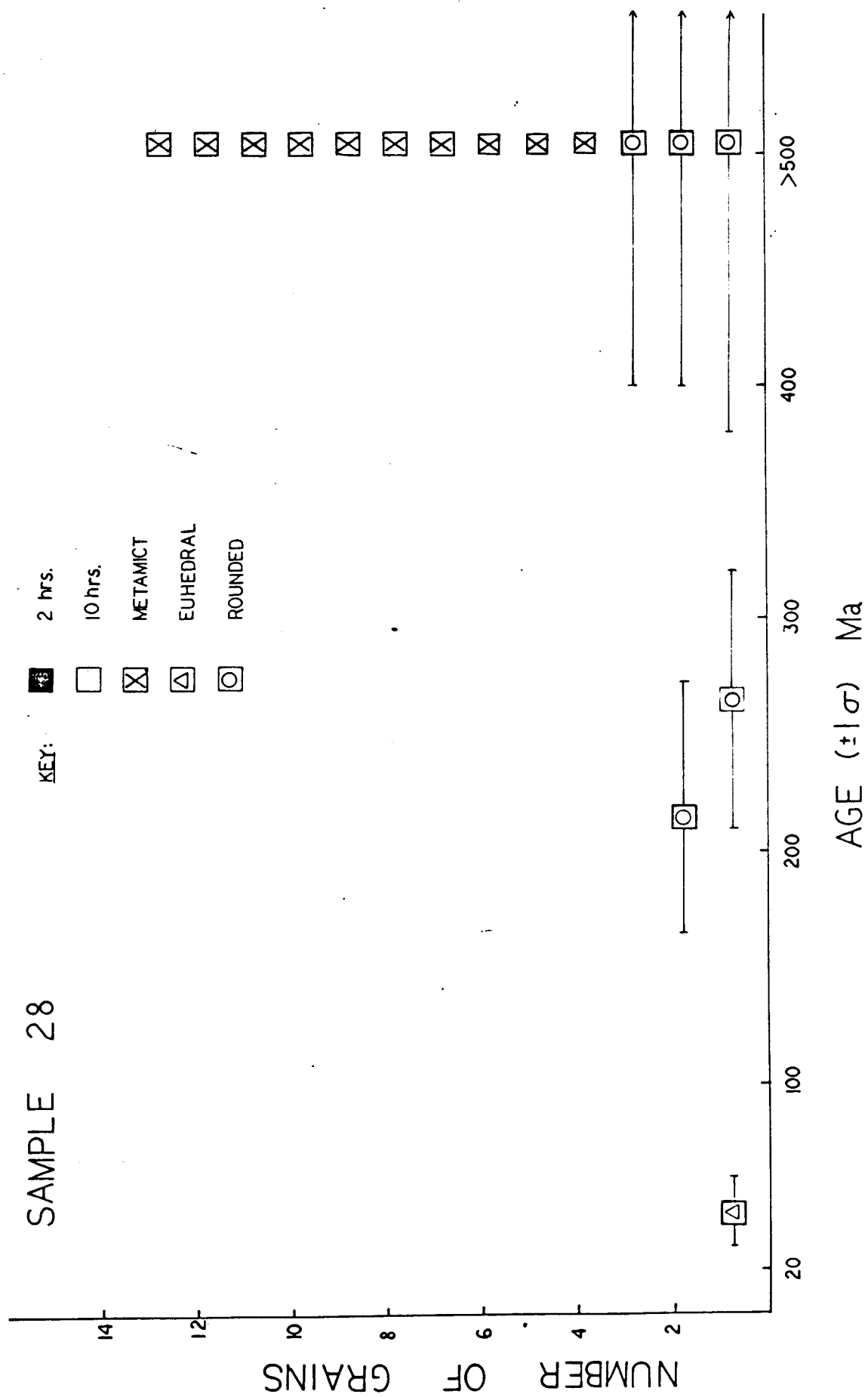
KEY:

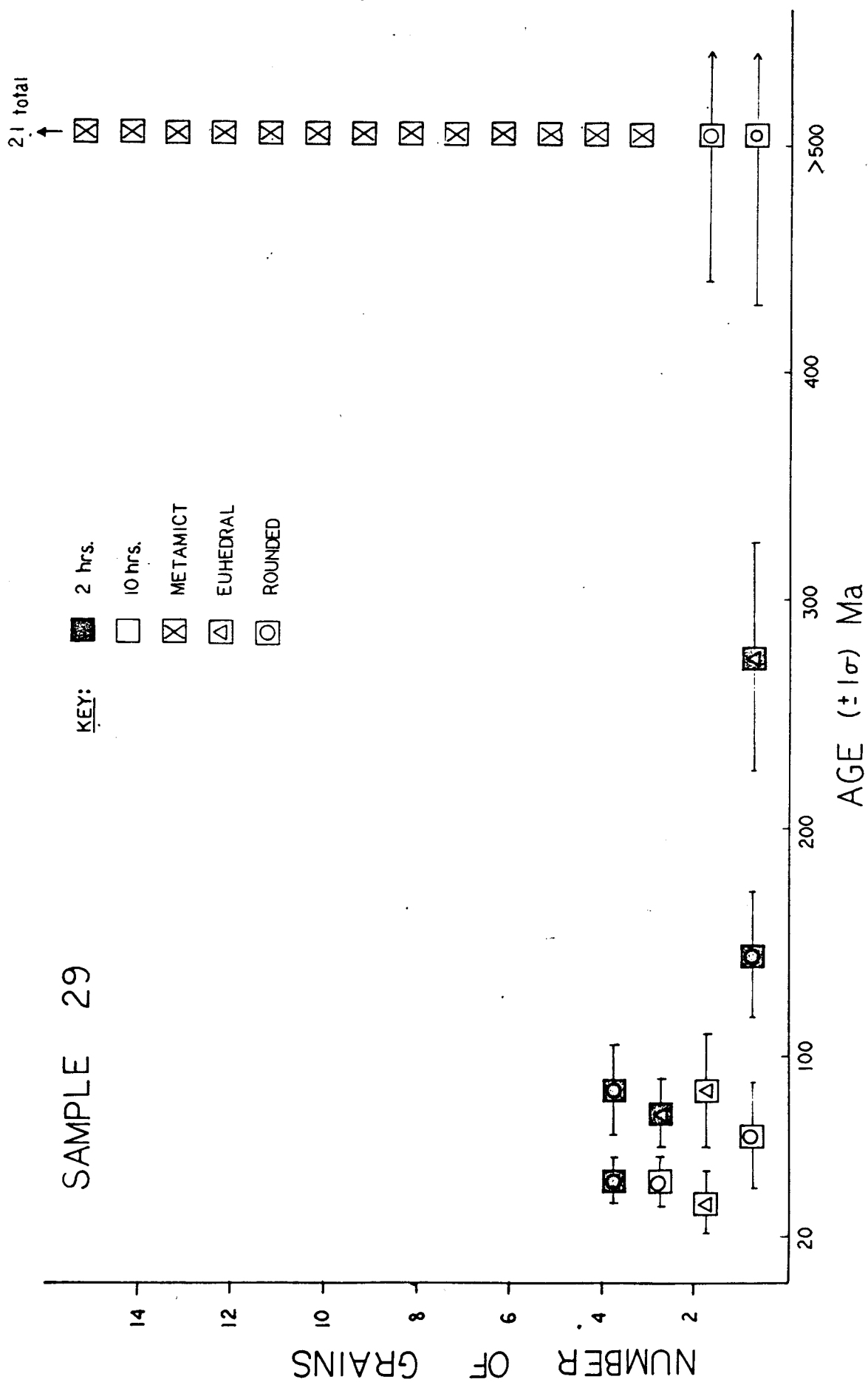
2 hrs.  10 hrs. 

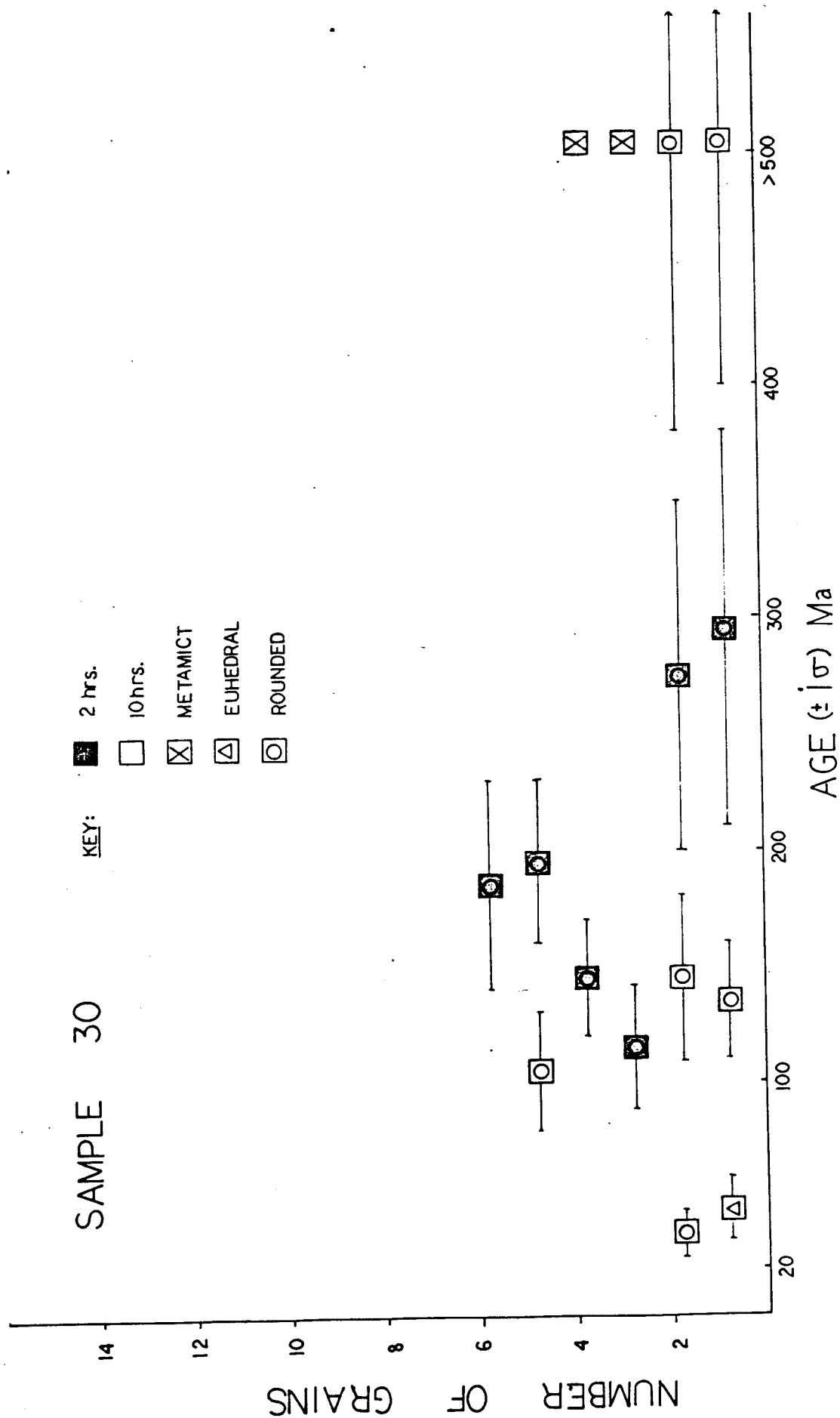
METAMICT  EUHEDRAL  ROUNDED 

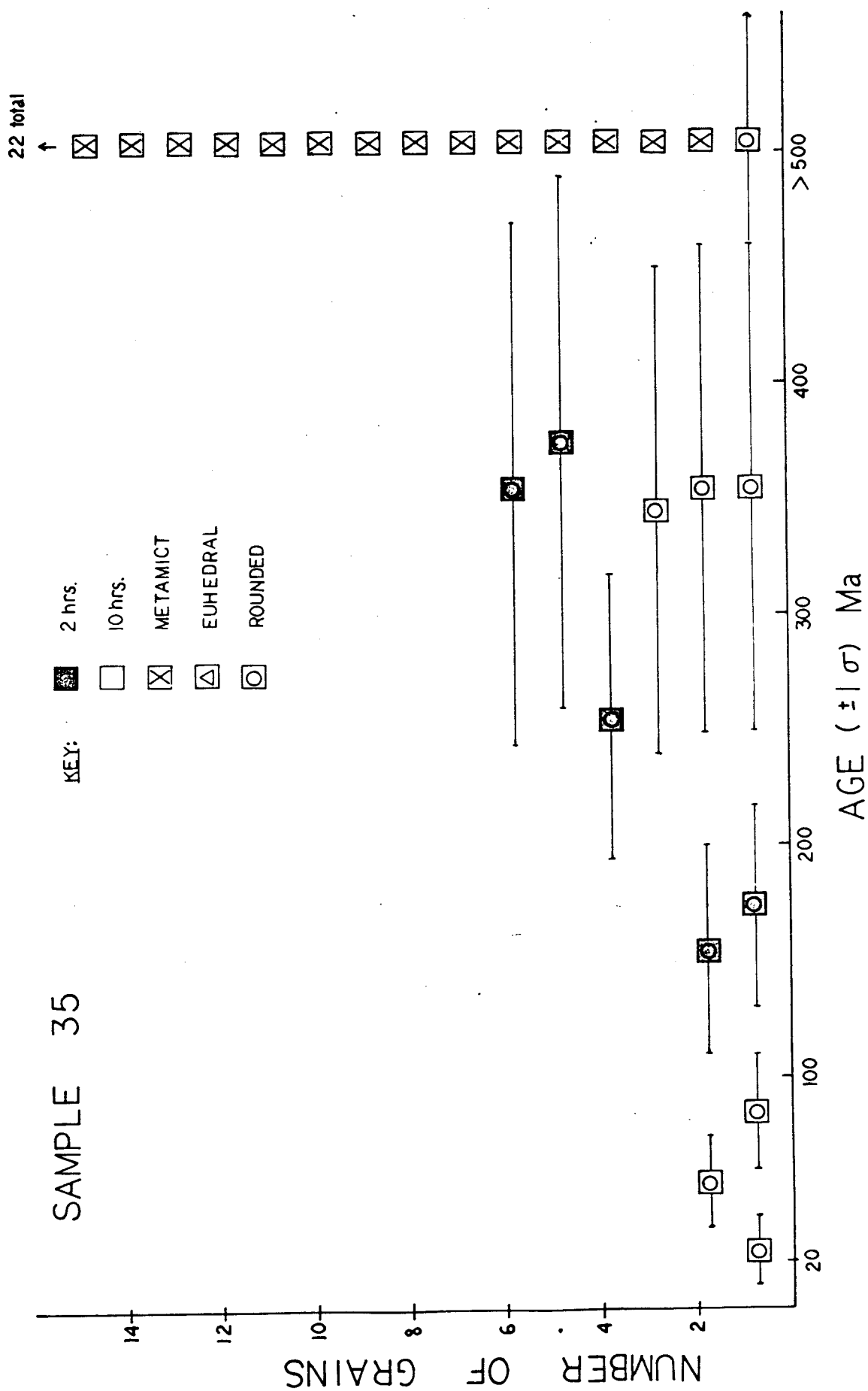












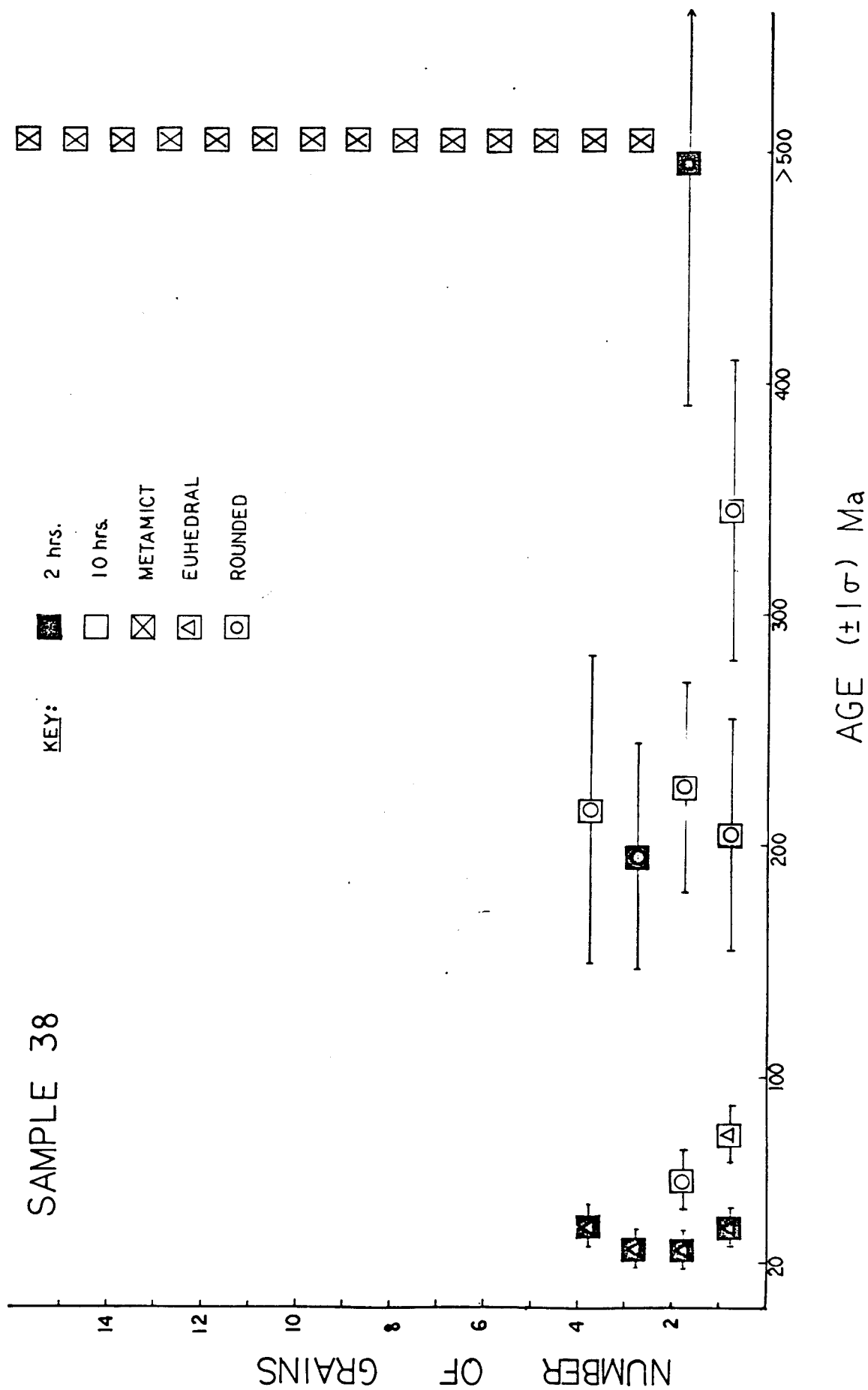
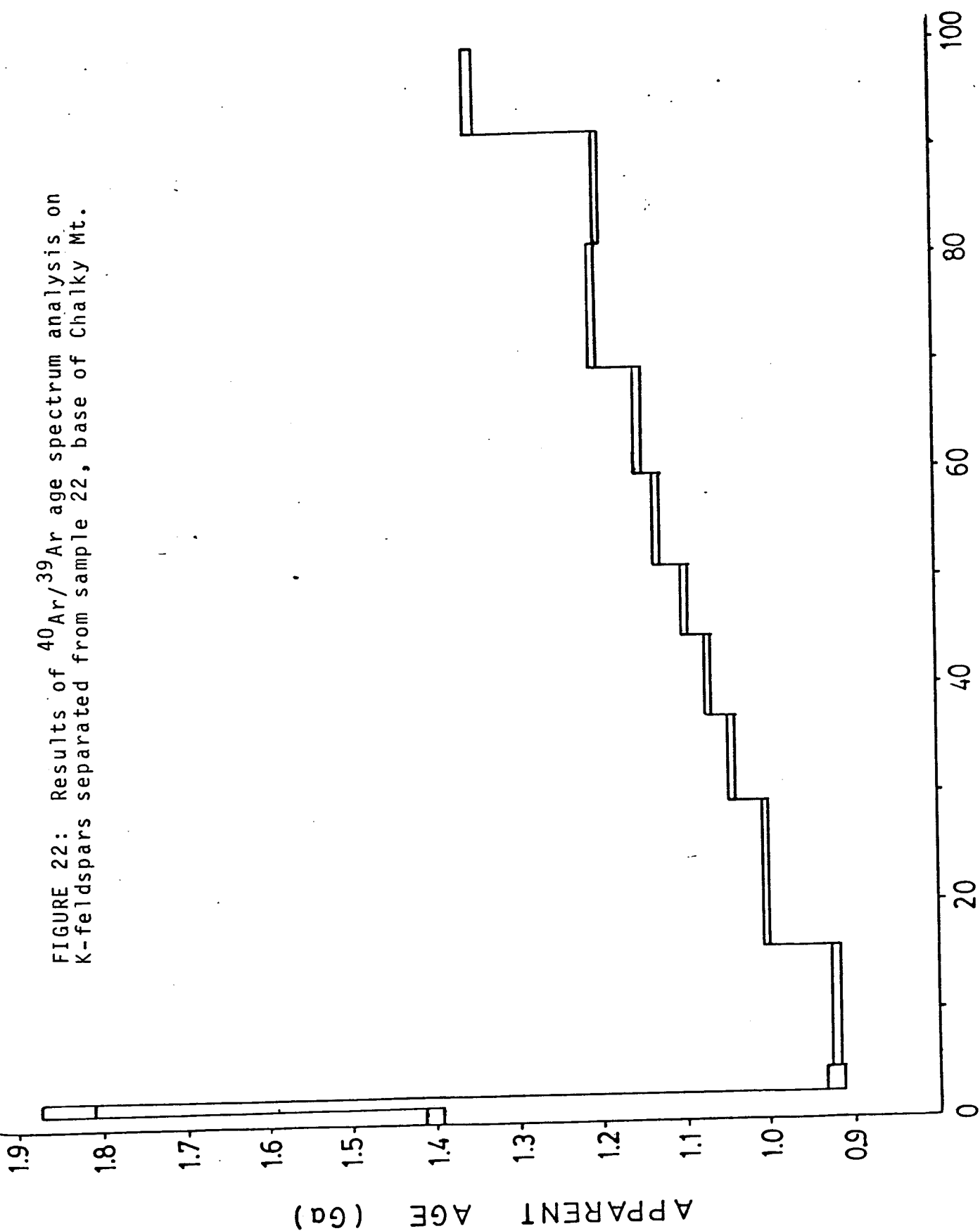


FIGURE 22: Results of $^{40}\text{Ar}/^{39}\text{Ar}$ age spectrum analysis on K-feldspars separated from sample 22, base of Chalky Mt.



% ^{39}Ar RELEASED

TABLE III: Results of $^{40}\text{Ar}/^{39}\text{Ar}$ age spectrum analysis on K-feldspars from sample 22, base of Chalky Mt., Barbados.

Temp (°C)	$^{40}\text{Ar}/^{39}\text{Ar}$	$^{37}\text{Ar}/^{39}\text{Ar}^1$ ($\times 10^{-3}$)	$^{36}\text{Ar}/^{39}\text{Ar}^3$ ($\times 10^{-3}$)	$^{39}\text{Ar}_K^4$ ($\times 10^{-14}$ mol)	$^{39}\text{Ar}_K$ (%)	$^{40}\text{Ar}^{*2}$ (%)	$^{40}\text{Ar}^*/^{39}\text{Ar}_K$	Age ± 1 s.d. (Ma)
BARB 22 K-spar (J = 0.007250; wt. = 0.10722 g)								
450	189.6	12.67	90.71	1.69	1.57	84.8	162.8	1406. ± 7 .
530	259.7	17.50	48.18	0.68	2.20	92.4	245.5	1840. ± 30 .
620	99.64	15.23	24.53	2.72	4.73	91.3	92.36	924.7 ± 8.0
710	93.32	10.56	3.563	11.8	15.7	98.5	92.23	923.8 ± 1.3
800	103.4	8.418	1.423	14.9	29.5	99.3	102.9	1005.6 ± 1.8
850	108.7	8.205	2.667	8.63	37.5	98.8	107.9	1042.4 ± 1.7
900	111.6	3.697	1.788	7.97	44.9	99.0	111.0	1065.4 ± 1.4
960	121.2	5.054	18.00	6.94	51.3	95.1	115.8	1099.9 ± 3.0
1020	120.0	8.616	2.938	8.74	59.4	98.9	119.1	1122.9 ± 2.2
1090	124.6	9.947	4.483	11.4	70.0	98.6	123.3	1151.9 ± 2.6
1150	133.3	9.660	8.158	12.1	81.2	97.9	130.9	1203.6 ± 2.8
1210	132.7	9.990	7.858	11.6	92.0	98.0	130.3	1200.2 ± 1.2
1350	161.6	20.20	29.27	8.52	100.0	94.4	152.8	1345.7 ± 2.9

¹ Corrected for decay of ^{37}Ar .

² Includes extraction blank.

³ Blank corrected.

⁴ Calculated from mass spectrometer sensitivity.

CHAPTER IV: PROVENANCE

Introduction

The source of the Scotland sediments of Barbados has long been a topic of debate (e.g., Senn, 1940; Dickey, 1980; Pudsey and Reading, 1982; Westbrook, 1982; Speed, 1983). Based on the mineralogy of the sands it has been proposed that the sediments were derived in large part from a metamorphic terrane in South America. The question that remains unanswered and that has implications for the tectonic history of the area is: Where in South America? The data presented herein marks a early attempt to gain insight into the provenance of sediments using isotopic techniques (e.g., Naeser et al., 1981; Harrison and Bé, 1983). A meaningful interpretation of bulk ages for detrital minerals in an area as complex as the southern Caribbean is rarely possible. However, apparent trends of single crystal ages may assist in understanding the source characteristics.

An obstacle in the interpretation of fission track results from Barbados is the paucity of isotopic data relating to the thermal history of northern South America. At present, the age ranges reported herein can only be used to distinguish between younger uplifted areas of northern South America and material derived from much older plutonic areas of South America.

Fission Track Age Interpretations

The retention of fission tracks in any mineral is a function of its cooling history. The closure temperature (T_c) corresponds to a temperature at which, theoretically, all the tracks become stable. For

zircons it has been estimated at approximately 200°C (Harrison et al., 1979; Hurford, 1984). Closure temperature varies between minerals and changes as a function of cooling rate and possibly radiation history. Thus T_c for areas that have been rapidly uplifted (ie. cooled quickly) will be high compared to that from a slowly cooled terrane.

In areas that have experienced complex thermal histories, fission track ages may represent:

- 1) the original cooling or crystallization ages of plutonic or volcanic rocks;
- 2) partial or complete annealing related to a thermal event;
- 3) regional uplift (ie., time since rock has been raised above the T_c isotherm); or
- 4) combinations of the above.

Clearly the only temporal information available from these results is related to the late stage cooling history of the source regions.

The youngest population reported for the Scotland sandstones (Tables 13-21, Chapter III) may reflect a variety of source areas. Ash falls from the Aves Ridge, active in latest Cretaceous to Paleocene time (Fox and Heezen, 1971) and Lesser Antillean ash falls (Eocene-early Miocene) may have contributed to this population. The ~~Netherland~~-Venezuelan Antilles island arc, active in the Cretaceous (Maresch, 1974) may also be a source for zircons. Zircon fission track ages from the western Caribbean Mountains of Venezuela yield ages that cluster around 20 Ma (Kohn et al., 1984) suggesting uplift of this area at that time and indicates a possible source of sediment.

While it is not clear what source area the 200-350 Ma population was derived from, these ages may reflect partially annealed cratonic

material. As areas are being uplifted zircons will cool to a critical temperature before track retention exceeds track annealing. Cratonic areas of South America cooled below 200 °C approximately 1 Ga ago thereby enabling fission tracks to begin to be retained. Uplifted areas in South America cooled later than cratonic areas, thus zircons will yield younger ages. The 200-350 Ma population may also reflect an Andean component that formed when South America and North America collided approximately 280 Ma ago (Figure 23; Pindell and Dewey, 1982) or a Triassic rifting event 200 Ma ago (Burke et al., 1978; 1984).

The oldest fission track ages (>500 Ma) from zircons of the Scotland sandstones very likely reflect material derived from the South American craton. $^{40}\text{Ar}/^{39}\text{Ar}$ age spectrum analysis of detrital feldspars from sample 22 (Table 22) provides additional evidence of a cratonic source for these sediments. Isotopic data from areas of the Guayana shield give ages that correspond to the oldest populations reported here (>500 Ma). Specifically, an $^{40}\text{Ar}/^{39}\text{Ar}$ age spectra of K-feldspars from the Encrucijada pluton of the Imtaca Complex yielded ages between 1.1 and 1.4 Ga (Onstott et al., 1984; Figure 24). Spinel separated from the Los Pijiquaos Pluton, Venezuela gave ages of 530 \pm 50 Ma (Barry Kohn, personal communication to Mark Harrison; Figure 24). The zircons separated from the pluton were metamict and therefore not datable. Based on age constraints discussed above, the source area for the Scotland sediments must include a part of the Guayana shield, uplifted areas of South America, and the Lesser Antilles volcanic arc.

Maracaibo Region of Venezuela

It has been proposed that the source area for Barbados sediments

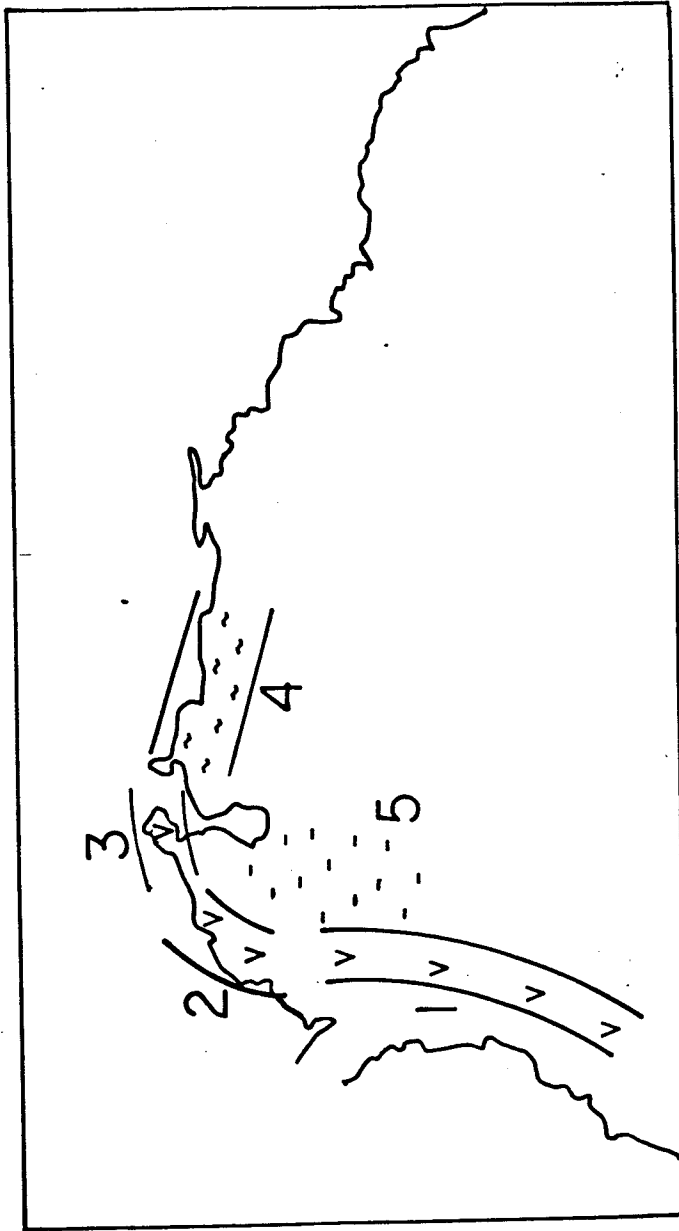
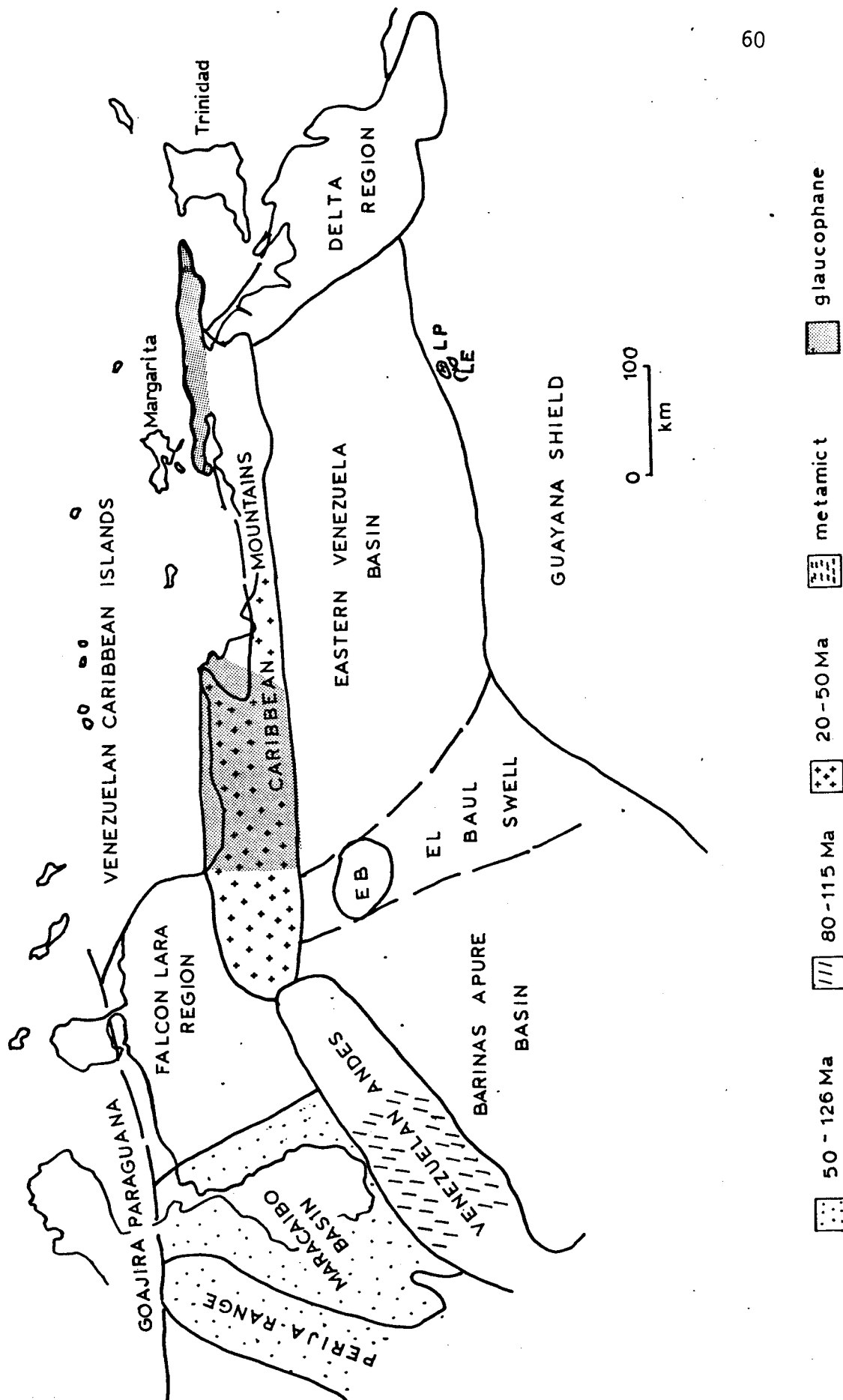


Figure 23; Late Paleozoic Terrains of Northern South America
 1= Cordillera Central (arc); 2= Sierra Nevada de Santa Marta
 arc; 3= Guajira Peninsula (arc); 4= Deformed Granites and
 Gneisses of Venezuela; 5= Shallow water Seaway Behind Late
 Paleozoic Arc, Similar to Java Sea (Figure 7, Pindell, 1981)

Figure 24: Geomorphological provinces of northern Venezuela (after Feo-Codecido, 1984). Patterns indicate previously reported zircon fission track ages (Shagam et al., 1984; Kohn et al., 1984). Shading indicates distribution of glaucophane (Gonzalez de Juano, 1980). Because the sedimentary wedge contains glaucophane, it is implied that the river draining the continent came out in an area between the Araya/Paria peninsula and the western Caribbean Mountains.



was a huge deltaic complex active in the Eocene in the circum-Maracaibo region of Venezuela (Senn, 1940; Dickey, 1980). This proposal implies that the Caribbean plate moved approximately 1100 km with respect to South America since Eocene time (approximately 2.2 cm/yr). Restored isopach and facies maps for the Lower Eocene of the Maracaibo region indicate the ancestral Magdalena- Catatumba river system formed a huge delta in this area (Forero, 1974). Northeast of Maracaibo a well-developed trough formed, and the Trujillo Fm. (consisting of deep marine shales and turbidites) and the Pauji Fm. (marine shales) were deposited in lower-mid Eocene (Forero, 1974). Zircons derived from an area of the Venezuelan Andes south of Maracaibo Basin yielded ages ranging from 60-172 Ma with a strong grouping around 81-113 Ma (Kohn et al., 1984; Figure 24). The majority of results are believed to represent partially annealed zircons (mixed ages). Zircons ages reported from the circum-Maracaibo region range from 50-126 Ma (Shagam et al., 1984; Figure 24). Some of these ages are believed to reflect uplift of the area in the late Cretaceous to Paleocene. In general, zircon fission track ages reported to date from northwestern parts of South America represent material that has been partially annealed due to uplift of the area. Fission track ages greater than 170 Ma have not been reported from the circum- Maracaibo region. It is most important to note that results from this study do not show strong groupings similar to those characteristic of results of zircon fission track dating from the circum-Maracaibo region.

Present-day Orinoco River System

Another possible source is the area drained by the present day

Orinoco River. This river channel is largely carved into the basement rocks of the Guayana Shield and therefore most of this material would be expected to yield ages greater than 500 Ma. East-west river drainage developed in the Miocene and has resulted in the formation of the immense Orinoco river delta located off eastern Venezuela and SE Trinidad (Saunders, 1980). However, this would imply that the Lesser Antilles arc remained in the same position since, at least, the Oligocene and therefore is discounted as a possible source area.

Unare River System

The Unare river system which empties into the Caribbean sea has captured a considerable portion of mountain drainage which originally drained to the Orinoco River or eastward to the Orinoco delta (Hedberg, 1950; Figure 25). The Barcelona gap, Unare drainage system and sharp bends in the present day Orinoco River suggest that the proto-Orinoco may have flowed northward into the Caribbean sea during earlier times. However, there is little information regarding the paleogeography between the Cordillera de la Costa and Araya- Paria Peninsula.

South of this area is the eastern Venezuelan basin which is filled with km of Mesozoic and Cenozoic sediments. The exact origin of this basin is not known. Subsidence began in the late Cretaceous, and marine and brackish water sediments were deposited. A regional unconformity exists in the mid-Eocene. A second period of deposition began in the late Eocene and extended through the Miocene. During this time 10 km of marine and brackish water deposits of the Santa Ines Fm were deposited in the basin. The axis of deposition within the basin

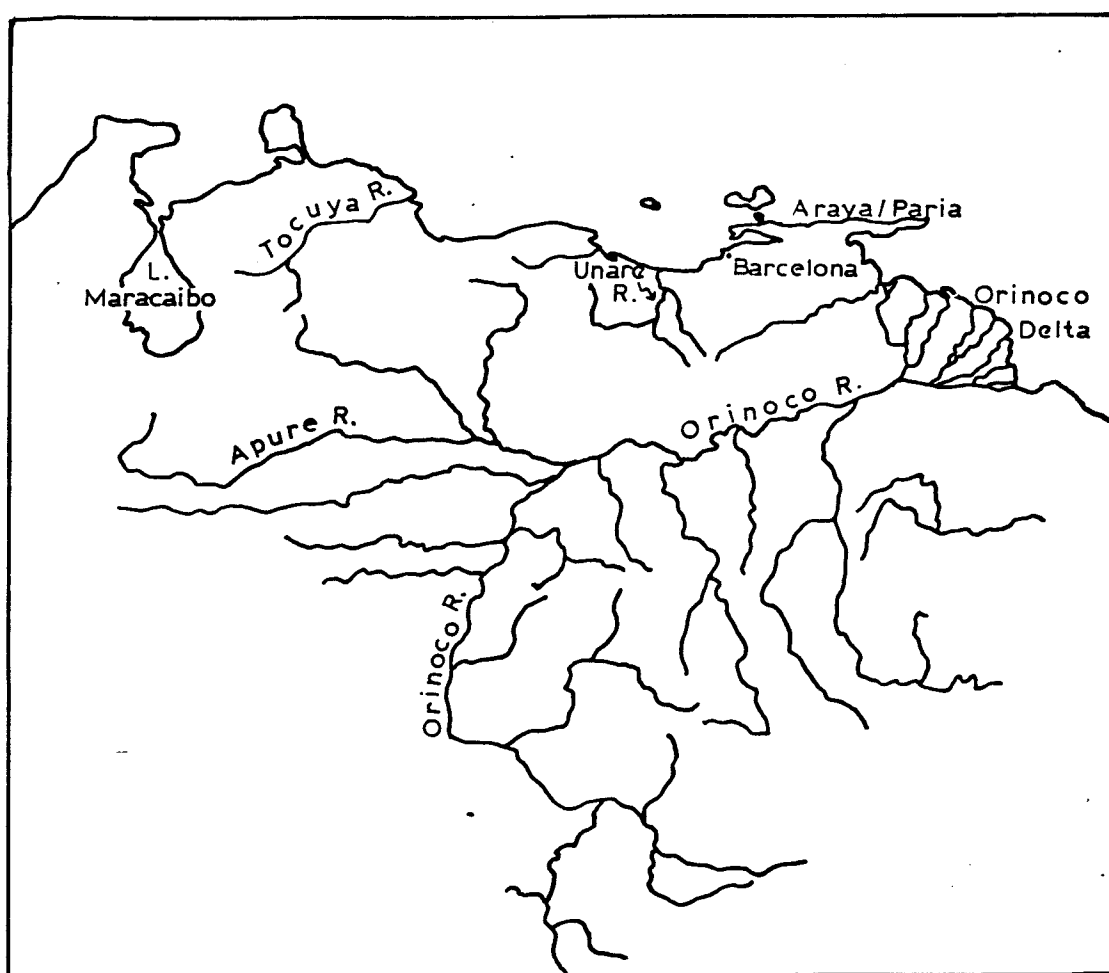


Figure 25: Distribution of active river systems in Venezuela.

migrated southward through time (Hedberg, 1950). In the late Miocene northeastern Venezuela was uplifted and deformed producing a regional unconformity. Brackish and fresh water deposits were deposited in lower to mid Pliocene times. The area was uplifted in Pliocene-Pleistocene times (Hedberg, 1950).

Zircon fission track results from the Caribbean Mountains west of the Barcelona gap yielded ages that cluster around 20 Ma suggesting uplift of this area at that time. We can speculate that in the late Oligocene, the zircon fission track ages of rocks exposed in this area would have been at least approximately 30 Ma.

Distribution of Glaucophane

Since there exists a distinct relationship between some metamorphic facies and geologic age (Miyashiro, 1973) the presence of glaucophane in the Scotland sandstones (Senn, 1940; Pudsey, 1981) may also provide information relating to the source area for these sediments. Glaucophane-schist facies rocks have been shown to be associated with younger Alpine-type orogenic belts in which rapid and large uplift is characteristic (Zwart, 1967). Blueschists are well known from the Caribbean Mountains of Venezuela. Specifically, they occur in the Antimano Fm of the Coastal Range Tectonic Belt, the Copey Fm of the Araya-Paria Peninsula, the Conopora Fm of the Caucagua-El Tinaco Belt and in ophiolites of the Villa de Cura Complex (Gonzalez de Juana et al., 1980) and in Tobago (Maxwell, 1948) (see Figure 24). The coastal ranges of Venezuela, west of Barcelona provide the metamorphic grade necessary to explain the heavy minerals present in the Scotland sandstones. Derivation of these minerals from points farther east

(i.e., Northern Range of Trinidad) is unlikely as these rocks have experienced lesser grades of metamorphism (Saunders, 1980).

Conclusion

It is possible that an outlet to the Caribbean sea developed in the northern mountain system (Cordillera de la Costa and Araya-Paria) west of Barcelona as a result of transverse faulting (Hedberg, 1947, 1950; Saunders, 1980). Thus drainage may have developed northwards flowing into the Caribbean sea. Such a river system would have drained much of the cratonic area to the south. Based on results from this study and the paleogeographic information presented above, it is proposed that the source area for the Scotland sediments of Barbados was an area of the Guayana Shield which was drained by the Unare (proto-Orinoco?) river system and deposited in a submarine fan north of the Unare depression.

CHAPTER V: ACCRETION IN THE LESSER ANTILLES ARC SYSTEM AS ILLUSTRATED
BY FISSION TRACK STUDIES OF THE SCOTLAND SANDSTONES, BARBADOS

"Several major problems hinder an understanding of the tectonic history of Barbados. One is the paucity of dating of rock deposition, especially of terrigenous lithotypes, within fault packets of the basal complex. Thus the absolute timing of structural events and stacking orders among accreted packets are poorly known." (Speed, 1983)

Introduction

Barbados occurs at the structural high of the forearc ridge associated with the Lesser Antilles arc system. It is expected that the age of sediments in the accretionary wedge decreases from the arc to the present day deformation front. Previous studies indicate that the easternmost portion of the prism (approximately 50 km west of the deformation front to the eastward limit of the deformation front) represents Neogene-Recent strata that have been accreted (Biju-Duval et al., 1982).

The structures observed in areas where active accretionary prisms are exposed (i.e., Barbados, Nias, Nicobar Islands, Kodiak Island) provide insight into processes occurring at convergent margins. Unfortunately Barbados represents a very small fraction of the accretionary wedge and it is doubtful whether structures observed on the island are representative of large-scale features associated with the movement of sediment within the wedge. It seems unlikely that the fault surfaces exposed in the Scotland district represent primary

surfaces of accretion or reactivated surfaces of accretion but rather, are a secondary result of large-scale movement in the prism. Furthermore, it is virtually impossible to distinguish between structures produced by accretionary processes and those produced as a result of, for example, ridge subduction. High water and clay content in the pelagic and hemipelagic deposits relative to trench sands probably facilitates overpressuring and the development of a decollement accompanying the offscraping of trench deposits (Moore et al., 1981). There is no evidence for advective flow within the accretionary prism of the Lesser Antilles arc system as proposed by Cowan and Silling (1978) and Cloos (1982).

Accretion as Illustrated in the Pre-coral Rock Section of Barbados

Complex structures associated with the Scotland units may be the result of sediment slumping, faulting while sediments were partially lithified and further complicated by the intrusion of mud diapirs. Because the sedimentary sequence and structural style varies between blocks (see map of Poole and Barker, 1983) it is assumed that blocks are separated by major faults. These faults can not be readily observed at outcrop, therefore the dip and sense of movement in many cases is unknown. Abrupt changes in bedding and structural style and nearly straight scarps that trend uphill and downhill are the most direct evidence for the presence of faults between blocks. Minimum age of faulting is estimated as pre-Pleistocene based on the fact that faults do not penetrate the coral reef cap. If the Scotland beds are as young as late Oligocene as proposed here, the maximum age of faulting may be early Miocene, not Eocene as previously suggested

(Speed, 1983).

Compared to the Scotland units, the Oceanic formation is substantially less deformed. Undulating anticlines and synclines and normal faults with minor displacements are common. The Oceanic Fm occurs in fault slices largely overlying the thrust slices of the Scotland units. Thus the Oceanics form a structural part of the accretionary wedge (Saunders, 1980).

The structures present in the Pleistocene coral reef terraces have not been examined in detail. Very little deformation, consisting mainly of joints and features associated with karst development, is present. Joints and faults are vertical to subvertical and strike dominantly NW-SE.

Scotland/Oceanic Contact

Senn (1940) stated that the Oceanic Fm lies with strong angular unconformity on the Scotland beds. He dated the unconformity as post mid-Eocene and pre-uppermost Eocene corresponding to what was believed to be the age of the rocks at that time. The exact nature of this contact has long been debated because it can not be observed directly. Pudsey and Reading (1982) claim that the contact is unconformable in places, but suggest the unconformity may have been a plane of movement during subsequent deformation. Other workers (Speed and Larue, 1982) claim the contact is a thrust surface and interpret it to be a primary surface of accretion or reactivated surface of accretion.

In several areas, the Scotland units and the Oceanic Fm are found juxtaposed presumably due to movement on faults. The best exposure of this contact is at Cattlewash where a sliver of the Oceanic Fm is atop

severely faulted Scotland beds (Figure 26). Although close viewing was not possible due to the precipitous cliffside in which this feature is exposed, Pudsey and Reading (1982) maintain that vertical burrows can be seen at the contact. Vertical burrows were observed in the mudstones of the Scotland beds, at this locality, but not at the contact. The structure at this locality is further complicated because the Oceanic and Scotland rocks form a faulted slice within the Joes River unit. At several other areas (ie., Bath, Congor Rocks, Skeetes Bay, and north of Bathsheba) the contact is not visible but changes in bedding orientation can be observed from the Scotland beds to the Oceanic Fm.

Recent work by Saunders et al., (1984) indicates that the Bath cliffs section of the Oceanic Fm ranges in age from late middle Eocene to early Oligocene. Microtektites separated from the mid-section yielded ages of 35 Ma (Billy Glass, per. comm. to Mark Harrison). Results presented here support the proposal that the late mid-Eocene - early Oligocene Oceanic Fm has overthrust the Eocene(?) - late Oligocene Scotland beds. Additional evidence supporting this proposal comes from seismic profiles of deformed forearc basin sediments on the flanks of the Tobago Trough. The Oceanic Fm most likely represents forearc basin deposits or upper slope basin deposits that were thrust over accreted Scotland sediments with motion being concentrated along zones of weakness between competent and incompetent beds (Figure 28).

Anomalous Structural Trend

Structures, in general, on Barbados trend approximately N60E which is anomalous with respect to the present-day N-S trend of the island



Figure 26: Sliver of Oceanic Fm atop severely faulted Scotland beds. Locality: Cattlewash.

arc. Several ideas have been proposed to explain this anomalous trend.

Seismic reflection profiles and a linear positive gravity anomaly led Westbrook (1975;1982) to suggest that a ridge may have been obliquely subducted at $13^{\circ}55'N$. If a ridge trending 290° was subducted, it would have caused sediments to build up to the south of the ridge resulting in compressional structures subparallel to the ridge. Thus oblique structural trends may be produced without changing the orientation of the tectonic setting. This proposal may help explain the southward dipping paleoslope on which the Oceanic Fm was deposited (Lohman,1974). Several authors (Bowin, 1976; Vierbuchen, 1979; Burke et al., 1984) have suggested that the Caribbean/South American plate boundary is a broad zone of deformation where right-lateral, strike-slip motion has played a major role in Tertiary times. The anomalous structural trend may be the result of secondary compression associated with right-lateral strike-slip motion (Kevin Burke, per. comm.). Extensional features striking NW-SE in the Coral rock section exposed on the island may also be related to strike-slip motion. Speed (1983) has suggested that the anomalous trend is a result of a differently oriented subduction zone. It seems most likely that this trend is a result of ridge subduction and/or secondary compression associated with a plate boundary zone.

Another intriguing question is: Why is Barbados the only portion of the enormous ridge complex exposed above sea level? Subduction of an oceanic transform or ridge may have uplifted this particular area (Westbrook, 1975). Another minor contributing factor may have been the rising mud diapirs of the Joes River Fm.

Figure 27 summarizes the tectonic framework in which the Scotland

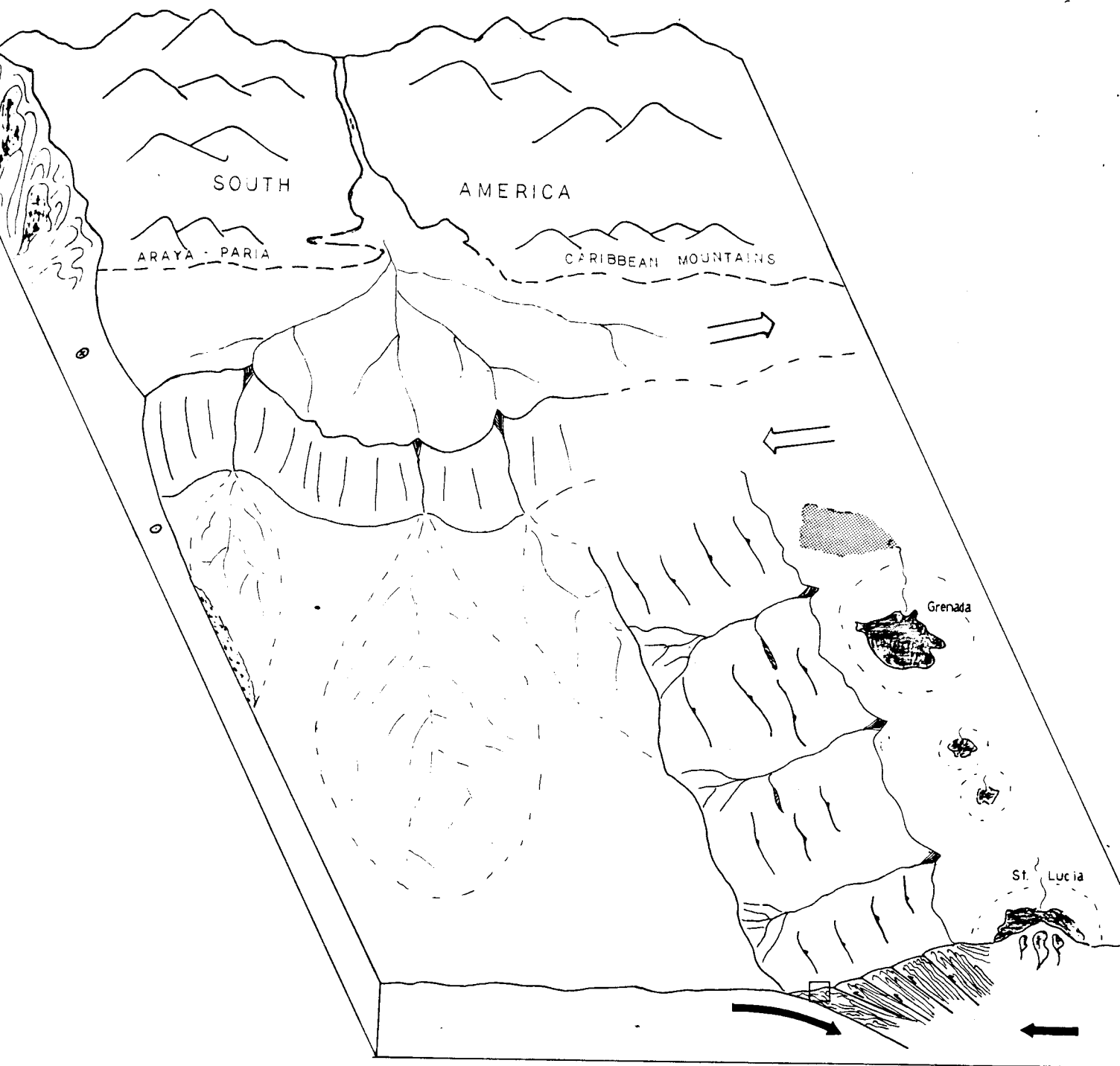


Figure 27: Schematic representation of South American/Caribbean plate boundary zone at end of the Oligocene depicting environment of deposition and source areas for Scotland sediments of Barbados. ☐ represents sediments that will form the Scotland rocks of Barbados.



Figure 28: Insert of Figure 27 showing close-up view of accreted Scotland sediments and overlying Oceanic upper slope basin deposits.

sediments of Barbados were deposited. The geologic history of the island begins with the deposition of the Scotland sediments in a submarine fan, abyssal cone or directly into the trench during Eocene(?)–late Oligocene. Pudsey (1981) has proposed that the Scotland units represent outer fan deposits and mid-fan sediments with coarser sands being channel fill. At approximately the same time or slightly earlier (late, mid-Eocene–early Oligocene) Oceanics were deposited in a nascent forearc basin or in secondary basins formed on rising thrust slices of the accretionary wedge. During early Miocene, the Bissex Hill Fm was deposited on top of the Oceanics (Saunders, 1973). The Joes River unit was intruded during post mid-Miocene time (Poole and Barker, 1983) incorporating blocks of Scotland rocks and Oceanic Fm within it. During Pleistocene to Recent times there was a continued widening of the prism as material was incorporated into the accretionary wedge. Coral reef terraces formed as a result of continued uplift, possibly due to ridge subduction. Uplifted Pleistocene reef terraces represent eustatic high sea levels superimposed on gradual and continuous uplift of the island (Mesolella et al., 1969, 1970).

Tectonic Implications of Fission Track Results

Results of this study indicate that the source areas for these sediments must include a portion of the Guayana shield and uplifted areas of northern South America. It is proposed that at the time the Scotland sediments were deposited, the deformation front of the accretionary wedge was located north of the Unare depression (Figure 27). This would imply that the deformation front has moved

approximately 500 km east to its present position since late Oligocene (1.8 cm/yr). Plate reconstructions of the Caribbean (Pindell and Dewey, 1982) place the deformation front of the accretionary wedge at approximately this position during late Oligocene-early Miocene lending further support to this proposal (Figure 29).

Data presented here do not provide information concerning relative movement between the Caribbean and South American plates during the Cenozoic. A study (in progress) to date the Tufton Hall Fm of Grenada (the westernmost exposure of accreted sediments) using fission track techniques may provide additional constraints on the source areas for the sediments of the accretionary wedge.

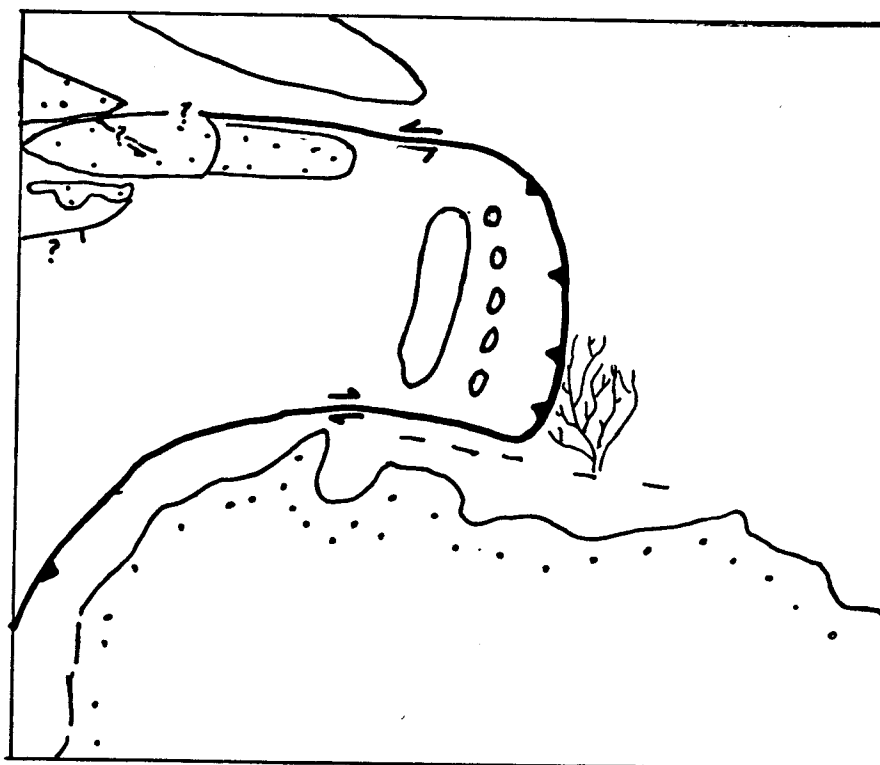


Figure 29: Caribbean plate boundary at approximately 28 Ma. Barbed line indicates position of deformation front (after Pindell, 1981). Suggested position of delta that is to be incorporated into the accretionary prism is shown to the right of the deformation front.

REFERENCES

- Barker, L.H., and E.G. Poole, 1983, The Geology and Mineral Resource Assessment of the Island of Barbados, Barbados Govt. Printing Office, pp. 1-109.
- Bender, M.L., R.G. Fairbanks, F.W. Taylor, R.K. Matthews, J.G. Goddard and W.S. Broecker, 1979, Uranium-series dating of the Pleistocene reef tracts of Barbados, West Indies, Geo. Soc. America Bull., Part I, Vol. 90, pp. 577-594.
- Biju-Duval, B., A. Mascle, L. Montadert and J. Wanneson, 1978, Seismic Investigations in the Colombia, Venezuela and Grenada Basins, and on the Barbados Ridge for Future IPOD drilling, Geologie en Mijnbouw, Vol. 57(2), pp. 105-116.
- Biju-Duval, B., P. LeQuellec, A. Mascle, V. Renard and P. Valery, 1982, Multibeam Bathymetric Survey and high Resolution Seismic Investigations on the Barbados Ridge Complex (Eastern Caribbean): A Key to the Knowledge and Interpretation of an Accretionary Wedge, Tectonophysics, Vol. 86, pp. 275-304.
- Bonini, W.E., 1984, The Caribbean-South American plate boundary and regional tectonics, Geo. Soc. America Memoir 162 (in press).
- Bowin, C., 1976, Caribbean Gravity Field and Plate Tectonics, Geo. Soc. America Special Paper 169, pp. 1-79.
- Brown, G.M., J.G. Holland, H. Sigurdsson, J.F. Tomblin and R.J. Arculus, 1977, Geochemistry of the Lesser Antiles volcanic island arc, Geochimica et Cosmochimica Acta, Vol. 41, pp. 785-801.
- Burke, K., P.J. Fox and A.M.C. Sengor, 1978, Buoyant Ocean Floor and the Evolution of the Caribbean, Jour. Geophys. Research, Vol. 83, No. B8, pp. 3949-3954.
- Burke, K., C. Cooper, J.F. Dewey, P. Mann and J.L. Pindell, 1984, Caribbean tectonics and relative plate motions, Geo. Soc. America Memoir 162, pp. 31-63.
- Carpenter, B.S., and G.M. Reimer, 1974, Calibrated Glass Standards for Fission Track Use, Natl. Bureau of Standards Special Publication 260-49, U.S. Dept. of Commerce, Washington, DC, pp. 1-27.
- Caudri, C.M., 1972, The larger Foraminifera of the Scotland District of Barbados, Eclog. Geol. Helv., Vol. 65, pp. 221-234.
- Chase, R.L., and E.T. Bunce, 1969, Underthrusting of the Eastern Margin of the Antilles by the Floor of the Western North Atlantic Ocean and Origin of the Barbados Ridge, Jour. Geophys. Research, Vol. 74, pp. 1413-1420.

- Chen, A.T., C. Frolich and G.V. Latham, 1982, Seismicity of the Forearc Marginal Wedge (Accretionary Prism), Jour. Geophys. Research, Vol. 87, No. B5, pp. 3679-3690.
- Cloos, M., 1982, Flow Melanges: Numerical Modeling and Geologic Constraints on their Origin in the Franciscan Subduction Complex, California, Geo. Soc. America Bull., Vol. 93, pp. 330-345.
- Cowan, D.S. and R.M. Silling, 1978, A Dynamic Sealed Model of Accretion at Trenches and its implications for the tectonic evolution of subduction complexes, Jour. Geophys. Research, Vol. 83, No. B11, pp. 5389-6291.
- Dickey, P.A., 1980, Barbados as a Fragment of South America Ripped off by Continental Drift, paper presented at the 1980 Caribbean Conference.
- Fleischer, R.L., P.B. Price and R.M. Walker, 1975, Nuclear Tracks in Solids: Principles and Applications, Univ. of California Press, 605 pp.
- Forero, O.E., 1974, The Eocene of Northwestern South America, Univ. of Tulsa, Oklahoma, unpublished MS Thesis.
- Fox, P.J., E. Schreiber and B.C. Heezen, 1971, The Geology of the Caribbean Crust: Tertiary Sediments, Granitic and Basic Rocks from the Aves Ridge, Tectonophysics, Vol. 12, pp. 89-109.
- Gleadow, A.J.W., and J.F. Lovering, 1974, The Effect of Weathering on Fission Track Dating, EPSL, Vol. 22, pp. 163-168.
- Gleadow, A.J.W., and J.F. Lovering, 1975, Fission Track Dating Methods, Pub. 3, School of Earth Sciences, Univ. of Melbourne, Parkville, Victoria, pp. 1-95.
- Gleadow, A.J.W., A.J. Hurford and R.D. Quaife, 1976, Fission Track Dating of Zircon: improved etching techniques, EPSL, Vol. 33, pp. 273-276.
- Gleadow, A.J.W., and J.F. Lovering, 1977, Geometry Factor for External Detectors in Fission Track Dating, Nuclear Track Detection, Vol. 1, No. 2, pp. 99-106.
- Gonzalez de Juana, C., J. Iturralde de Arozema and X. Picard Cadillat, 1980, Geologia de Venezuela y de Sus Cuencas Petroliferas Tomo, I and II, Caracas.
- Harrison, T.M., 1977, Fission Track, Potassium-Argon and Rubidium/Strontium Geochronology and Thermal History of the Coast Plutonic Complex, near Prince Rupert, B.C., unpublished BS Thesis, Dept. of Geological Sciences, Univ. of British Columbia.

- Harrison, T.M., R.L. Armstrong, C.W. Naeser and J.E. Harakal, 1979, Geochronology and thermal history of the Coast Plutonic Complex, near Prince Rupert, British Columbia, Vol. 16, No. 3 (Part I), pp. 400-410.
- Harrison, T.M., 1980, Thermal Histories from the $^{40}\text{Ar}/^{39}\text{Ar}$ Age Spectrum Method, Research School of Earth Sciences, Australian Natl. Univ., unpublished Ph.D. Thesis, 257 pp.
- Harrison, T.M. and I. McDougall, 1982, The thermal significance of potassium feldspar K-Ar ages inferred from $^{40}\text{Ar}/^{39}\text{Ar}$ age spectrum results, *Geochimica et Cosmochimica Acta*, Vol. 46, pp. 1811-1820.
- Harrison, T.M. and K. Be, 1983, $^{40}\text{Ar}/^{39}\text{Ar}$ age spectrum analysis of detrital microclines from the southern San Joaquin Basin, California: an approach to determining the thermal evolution of sedimentary basins, *EPSL*, Vol. 64, pp. 244-256.
- Hedberg, H.D., L.C. Sass and H.J. Funkhouser, 1947, Oil Fields of Greater Ofocina Area Central Anzoategui, Venezuela, *AAPG Bull.*, Vol. 31, No. 12, pp. 2089-2169.
- Hedberg, H.D., 1950, Geology of the Eastern Venezuela Basin (Anzoategui-Monagas-Sucre-Eastern Guarico Portion), *AAPG Bull.*, Vol. 61, No. 11, pp. 1173-1216.
- Hurford, A.J., 1984, On the closure temperature for fission tracks in zircon, *Abst. 4th International Fission Track Dating Workshop*, Troy, N.Y., p. 22.
- Johnson, N.M., V.E. McGee and C.W. Naeser, 1979, A Practical Method of Estimating Standard Error of Age in the Fission Track Dating Method, *Nuclear Tracks*, Vol. 3, No. 3, pp. 93-99.
- Jordan, T.H., 1975, The present-day motions of the Caribbean Plate, *Jour. Geophys. Research*, Vol. 80, No. 32, pp. 4433-4439.
- Jukes-Browne, A.J., and J.B. Harrison, 1891, The geology of Barbados, Part I - the coral-rocks of Barbados and other West-Indian islands, *Q.J. Geol. Soc. London*, Vol. 47, pp. 197-250.
- Karig, D.E., 1974, Evolution of Arc Systems in the Western Pacific, *Ann. Rev. Earth and Planetary Sciences*, Vol. 2, pp. 51-76.
- Karig, D.E., 1980, Material Transport within Accretionary Prisms and the "Knocker" Problem, *Jour. of Geology*, Vol. 88, pp. 27-39.
- Karig, D.E., J.G. Caldwell and E.M. Parmentier, 1976, Effects of Accretion on the Geometry of the Descending Lithosphere, *Jour. Geophys. Research*, Vol. 81, No. 35, pp. 6281-6291.
- Karig, D.E., and G.F. Sharman III, 1975, Subduction and Accretion in Trenches, *Geo. Soc. America Bull.*, Vol. 86, pp. 377-389.

- Kearey, P., 1974, Gravity and seismic reflection investigations into the crustal structure of the Aves Ridge, eastern Caribbean, *Geophys. J.R. Astr. Soc.*, 38, pp. 435-448.
- Kohn, B.P., R. Shagam and T. Subieta, 1984, Results and preliminary implications of sixteen fission-track ages from rocks of the western Caribbean Mountains, Venezuela, *Geo. Soc. America Memoir* 162, in press.
- Kohn, B.P., R. Shagam, P.O. Banks and L.A. Burkley, 1984, Mesozoic-Pleistocene fission-track ages on rocks of the Venezuelan Andes and their tectonic implications, *Geo. Soc. America Memoir* 162, in press.
- Larue, D.K., J. Schoonmaker, R. Schneider, M. Clark, J. Clark and R. Torrini, 1983, On Land Transect across Barbados, the crest of the Barbados Accretionary Prism: Quantifiable Diagenetic Properties and Hydrocarbon Potentials, *Geo. Soc. America Abstracts with Programs*, p. 623.
- Lawrence, S.R., L.H. Barker, and P. Payne, 1983, A geological and geophysical investigation of Barbados and the application of an accretionary prism model, 10th Carib. Geol. Conf., Cartagena, August 1983.
- Lohman, G.P., 1974, Paleo-oceanography of the Oceanic Formation, Barbados. Unpubl. Phd. thesis, Brown University.
- Maresch, M.V., 1974, Plate tectonic origin of the Caribbean Mountain System of northern South America: Discussion and proposal, *Geo. Soc. America Bull.*, 85, pp. 669-682.
- Maxwell, J.C., 1948, Geology of Tobago, British West Indies, *Geo. Soc of America Bull.*, v.59, p.801-854.
- Mesolella, D.J., R.K. Matthews, W.S. Broecker and D.L. Thurber, 1969, The astronomical theory of climatic change: Barbados data, *Jour. of Geology*, Vol. 77, pp. 250-274.
- Mesolella, K.J., H.A. Sealy and R.K. Matthews, 1970, Facies geometries within Pleistocene reefs of Barbados, West Indies, *AAPG Bull.*, Vol. 54, pp. 1899-1917.
- Miyashiro, A., 1973, *Metamorphism and Metamorphic Belts*, George Allen & Unwin Ltd., London, 492 p.
- Moore, G.F., and D.E. Karig, 1980, Structural Geology of Mias Island, Indonesia: Implications for Subduction Zone Tectonics, *American Journal of Science*, Vol. 280, pp. 193-223.

- Moore, C., J.S. Watkins, T.H. Shipley, K.J. McMillen, S.B. Bachman and C. Lundberg, 1982, Geology and tectonic evolution of a juvenile accretionary terrane along a truncated convergent margin: Synthesis of results from Leg 66 of the Deep Sea Drilling Project, southern Mexico, *Geo. Soc. America Bull.*, Vol. 93, pp. 847-861.
- Moore, J.C., J.S. Watkins and T.H. Shipley, 1981, Summary of Accretionary Processes, DSDP Leg 66: Offscraping, Underplaying, and Deformation of the Slope Apron, Initial Reports of the DSDP, Vol. 66, pp. 825-836.
- Naeser, C.W., A.J.W. Gleadow and G.A. Wagner, 1979, Standardization of fission-track data reports, *Nuclear Tracks*, Vol. 3, pp. 133-136.
- Naeser, C.W., 1979, Fission track dating and geologic annealing of fission tracks, in *Lectures in Isotope Geology*, E. Jager, J.C. Hunziker, eds., p.154-169.
- Naeser, C.W., 1981, The fading of fission tracks in the geologic environment - data from deep drill holes, *Nuclear Tracks*, v.5, p.248-250.
- Naeser, C.W., Zimmerman, R.A., and G.T. Cebula, 1981, Fission track dating of apatite and zircon: an interlaboratory comparison, *Nuclear Tracks*, v.5, p. 65-72.
- Onstott, T.C., R.B. Hargraves, D. York and C.M. Hall, 1984, Constraints on the motions of South American and African Shields during the Proterozoic: I. $^{40}\text{Ar}/^{39}\text{Ar}$ and paleomagnetic correlations between Venezuela and Liberia, *Geo. Soc. Am. Bull.*, v.95, no.9, p.1045-1054.
- Ostle, B. and R.W. Mensing, 1975, *Statistics in Research*, 3rd ed. Iowa State Univ. Press/Ames.
- Perez, O.J., and Y.P. Aggarwal, 1981, Present Day Tectonics of the Southeastern Caribbean and Northeastern Venezuela, *Jour. Geophys. Research*, Vol. 86, No. B11, pp. 10791-10804.
- Peter, G., and G.K. Westbrook, 1976, Tectonics of Southwestern North Atlantic and Barbados Ridge Complex, *AAPG Bull.*, Vol. 60, No. 7, pp. 1078-1106.
- Pindell, J., 1981, Permo-Triassic Reconstruction of Western Pangaea and the Evolution of the Gulf of Mexico-Caribbean Region, State Univ. of New York at Albany, unpublished MS Thesis, 121 pp.
- Pindell, J., and J.F. Dewey, 1982, Permo-Triassic Reconstruction of Western Pangaea and the Evolution of the Gulf of Mexico/Caribbean Region, *Tectonics*, Vol. 1, No. 2, pp. 179-211.
- Poole, E.G., and L.H. Barker, 1983, *Geology of Barbados*, 1:50,000, D.O.S., 1st ed., Office of Lands and Surveys, Bridgetown, Barbados.

- Pudsey, C.J., 1981, Sedimentation in the Ordovician of Western Ireland and the Territory of Barbados, West Indies, Univ. of Oxford, unpublished Ph.D. Thesis.
- Pudsey, C.J., and H.G. Reading, 1982, Sedimentology and Structure of the Scotland Group, Barbados, in *Trench-Forreard Geology*, Geo. Soc. of London Spec. Pub. No. 10, Blackwell Scientific Publications, London, pp. 291-308.
- Saunders, J.B., 1965, Field trip guide, Barbados, 4th Caribbean Geol. Congr., Trinidad, pp. 443-449.
- Saunders, J.B., 1973, Excursion No. 8: Margarita-Barbados, 2nd Latin American Conference, Caracas, Venezuela.
- Saunders, J.B., 1979, Field guide, Barbados, 4th Latin American Geol. Congr., Trinidad field trip I(J), pp. 73-88.
- Saunders, J.B., 1980, The development of the Caribbean with special reference to the southern margin and the Venezuela Basin in *Geologie des Chaines Alpines issues de la Tethys*, Aubouin, J., coordinator; et al., Fr. Bur. Rech. Geol. Minieres, Mem. no. 115, p. 238-243.
- Saunders, J.B., D. Bernoulli, E. Muller-Merz, H. Oberhansti, K. Perch-Nelson, W.R. Reidel, A. Sanfilippo and R. Torrini Jr., 1984, Stratigraphy of the late middle Eocene to early Oligocene in the Bath cliffs section, Barbados, W.I., *Micropaleontology*, in press.
- Scholl, D.W., R. VonHuene, J.L. Vallier and D.G. Howell, 1980, Sedimentary Masses and Concepts about Tectonic Processes at Underthrust Ocean Margins, *Geology*, Vol. 8, pp. 564-568.
- Scientific Party, Leg 78A, DSDP, Scraping off, subduction scrutinized, *Geotimes*, Oct. 1981.
- Senn, A., 1940, Paleogene of Barbados and its Bearing on History and Structure of Antillean-Caribbean Region, *AAPG Bull.*, Vol. 24, No. 9, pp. 1548-1610.
- Shagam, R., B.P. Kohn, P.O. Banks, L.E. Rodriguez and N. Pinentel, Tectonic Implications of Cretaceous-Pliocene fission-track ages from rocks of the circum-Maracaibo Basin region of western Venezuela and eastern Colombia, *Geo. Soc. America Special Paper* 162, in press.
- Smith, P.L., 1975, Tectonic History of Barbados and Implications for Shallow Subduction Processes, *Geolog. Soc. Amer. Abstracts with Programs*, Vol. 7, pp. 1276-1277.
- Speed, R.C., and D.K. Larue, 1982, Barbados: Architecture and Implications for Accretion, *Jour. Geophys. Research*, Vol. 87, No. B5, pp. 3633-3643.

- Speed, R.C., 1983, Structure of the accretionary complex of Barbados, I: Chalky Mt., Geo. Soc. America Bull., Vol. 94, pp. 92-116.
- Stein, S., J.F. Engeln and D.A. Wiens, 1982, Subduction Seismicity and Tectonics in the Lesser Antilles Arc, Jour. Geophys. Research, Vol. 87, No. B10, pp. 8642-8664.
- Steineck, D.L. and G. Murtha, 1979, Foraminiferal Paleobathymetry of Miocene Rocks, Barbados, Lesser Antilles, paper presented at the 4th Latin American Geological Conference, Port of Spain, Trinidad.
- Steinen, R.P., R.S. Harrison and K. Matthews, 1973, Eustatic Low Stand of Sea Level between 125,000 and 105,000 B.P.: Evidence from the Subsurface of Barbados, West Indies, Geo. Soc. America Bull., Vol. 84, pp. 63-70.
- Stride, A.H., R.H. Belderson and N.H. Kenyon, 1982, Structural Grain, Mud Volcanoes and other features on the Barbados Ridge Complex revealed by Gloria Long-Range Side-scan sonar. Marine Geology, Vol. 49, pp. 187-196.
- Sykes L.R. and Ewing, M., 1965, The seismicity of the Caribbean region, J. Geophys. Res., v.70, p.5065-5074.
- Uyeda, S., 1982, Subduction Zones: An Introduction to Comparative Subductology, Tectonophysics, Vol. 81, pp. 133-159.
- Velbel, M.A., Petrography of Subduction Zone Sandstones - a discussion, Jour. Sed. Petrol., Vol. 50, No. 1, pp. 303-304.
- Velbel, M.A., 1981, Phyllosilicate Authigenesis in sandstones of the Scotland Formation, Barbados, West Indies, Geo. Soc. America Abst. with Programs, Vol. 13, p. 572.
- Vierbuchen, R.C., Jr., 1979, The Tectonics of Northeastern Venezuela and the Southeastern Caribbean Sea, Princeton Univ., unpublished Ph.D. Thesis, 169 pp.
- Wadge, G. and K. Burke, 1983, Neogene Caribbean Plate Rotation and Associated Central American Tectonic Evolution, Tectonics, Vol. 2, No. 6, pp. 633-643.
- Wagner, G.A., 1972, The geological interpretation of fission track ages (abstract), Transactions of the American Nuclear Society, Vol. 15, p. 117.
- Westbrook, G.K., 1975, The Structure of the Crust and Upper Mantle in the Region of Barbados and the Lesser Antilles, Geophys. J.R. Ast. Soc., Vol. 43, pp. 201-242.

- Westbrook, G.K., 1982, Barbados Ridge Complex: Tectonics of a Mature Forearc System in Trench-Forearc Geology, Geo. Soc. of London Spec. Pub. No. 10, Blackwell Scientific Publications, London, pp. 275-290.
- Zwart, H.J., 1967, The duality of orogenic belts, Geol. Mijnbouw, v.46, p.283-309.

APPENDIX I: THEORY AND METHODS OF FISSION TRACK DATING

Introduction

The techniques used for fission track dating of geological materials have been developed largely through the efforts of Fleischer, Price, and Walker (1975). Fission track dating has been used to date time of extrusion of volcanic rocks and time of emplacement for shallow level plutons, to determine the provenance for sedimentary rocks, and in conjunction with annealing experiments, to determine the thermal history of rocks.

Theory

When a ^{238}U atom spontaneously fissions in nature it produces two fragments and liberates approximately 200 MeV of energy (Naeser, 1979). These highly charged fission fragments will travel through an insulating material and form a damage zone (approximately 15 μm long and 15 \AA in diameter) called a fission track. Figure 30 shows the currently accepted mechanism for the formation of fission tracks. Fission fragments pass through the crystal leaving positively charged atoms which then repel each other. If the mineral is etched with the proper chemical etchant, tracks become visible with the aid of an optical microscope at powers of 900-1250 x. The density of spontaneous tracks is a function of the age of the mineral and its uranium concentration. Thus, it is possible to observe the same spontaneous track density for a Cenozoic zircon with a high uranium concentration, and a pre-Cambrian zircon with a low uranium concentration. Tracks will be stable in insulating solids; conductors and semi-conductors

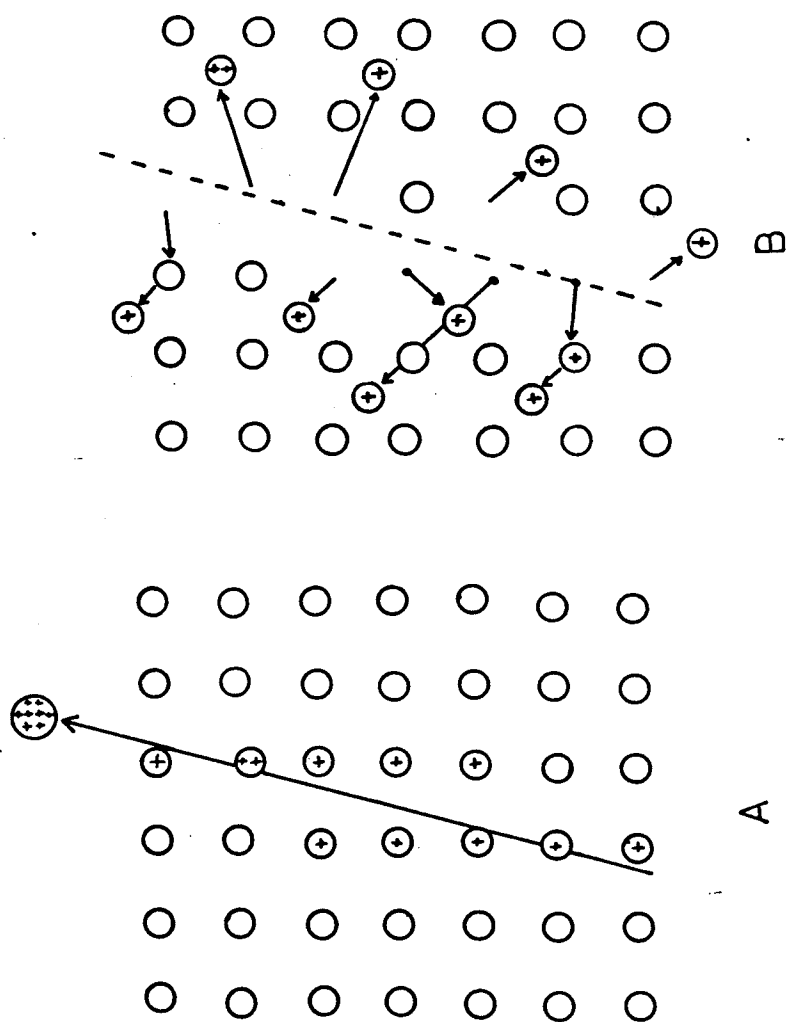


FIGURE 30: Track formation in a simple crystalline solid. A: The atoms have been ionized by the massive charged particle which has just passed. B: The mutual repulsion of the ions has separated them and forced them into the lattice. (courtesy of R.L. Fleisher, Naeser, 1979).

will not retain tracks because rapidly moving electrons will neutralize the charge zone. Preservation of fission tracks is temperature dependent. At high temperatures random atomic movement increases and atoms will diffuse back into the damaged zone. The closure temperature (Naeser, 1979) for zircons is approximately 200° over periods of geologic time. For each atom that spontaneously fissions, however, about one million atoms decay by alpha emission (Naeser, 1979) requiring an accounting for both modes of decay in the age equation. The fission track technique in essence allows microanalysis because an age can be determined for an individual mineral grain.

Age Equation

The derivation of the fission track equation is straightforward and described elsewhere (e.g., Gleadow and Lovering, 1975). In order to date a mineral using this technique, sufficient time must have elapsed so that a significant number of tracks have accumulated. To calculate an age it is necessary to determine the spontaneous track density and the uranium concentration of the mineral. The easiest way to determine the ^{238}U concentration is to induce a new set of tracks in the mineral by fissioning ^{235}U in a reactor. The age equation is:

$$t = \ln \left[1 + \left(\frac{\rho_s}{\rho_i} - \frac{\lambda_D \Phi I}{\lambda_F} \right) \right] \frac{1}{\lambda_D}$$

where t is the time (in years) elapsed since the mineral cooled below its annealing temperature and

ρ_s = spontaneous track density

ρ_i = induced track density

λ_D = total decay constant for ^{238}U

λ_F = decay constant for spontaneous fission for ^{238}U

$\bar{\Phi}$ = number of neutrons per cm^2 that pass through the
sample (neutron dose)

σ = cross-section for neutron reaction of ^{235}U
(i.e., size of U target)

I = atomic ratio $^{235}\text{U}/^{238}\text{U}$

Using a flux monitor which consists of a standard mineral of known age and knowing the time the sample was irradiated we can determine the ^{235}U concentration because the induced track density is a function of the time the sample was in the reactor and its uranium concentration. Multiplying the ^{235}U concentration by the constant $^{238}\text{U}/^{235}\text{U}$ it is possible to determine the ^{238}U concentration of the mineral.

Assumptions

In using this technique the following assumptions are made:

- 1) Only ^{238}U produces a significant number of spontaneous fission tracks. Although ^{235}U and ^{232}Th also spontaneously fission in nature their half lives are so long that we can neglect their contribution to the fission track density.
- 2) The spontaneous fission decay of ^{238}U atoms takes place at a constant rate (i.e., is independent of environmental factors).
- 3) $^{235}\text{U}/^{238}\text{U}$ is constant in nature (1/137.88).
- 4) All induced tracks are caused by the fission of ^{235}U in the reactor. ^{232}Th and ^{244}Pu will also fission but at much higher neutron energies. Provided that the flux is essentially thermal, this assumption is reasonable.

Experimental Methods

There are several methods used for the fission track dating of minerals. The most common are the population method and the external detector method. The population method involves splitting the sample with one split etched to reveal spontaneous tracks (and then counted), and the other split heated to temperatures which cause tracks to anneal. This later aliquant is then irradiated, etched to reveal the induced tracks and counted. This method can only be used if the sample being dated is known to have a constant uranium concentration. It also requires a minimum of several hundred grains.

Since the zircons within the samples collected had varying uranium concentrations, the external detector method was used. This method involves mounting, polishing and etching all the mineral grains. The sample is then covered with a low U mica detector and irradiated. ^{235}U atoms fissioning near the surface of the grain will bury fission fragments into the adjacent detector. After irradiation, the detector is etched and the induced tracks are counted. The spontaneous tracks are counted in the grain and induced tracks are counted in the mirror image produced in the detector. Etching efficiencies must be similar for mineral and detector or a correction must be made.

Sample Suitability and Location

Mineral grains must contain sufficient uranium concentration, be longer than one track length (15 μm) and be relatively free of inclusions and dislocations in order to be suitable for dating by this technique.

Eight samples were collected from the Scotland beds (see plate 1). The coarsest sands were chosen as these were expected to yield grains large enough for analysis. The Murphys member was not sampled due to lack of suitable sandstones within this unit. For each sample, 16 liters of material was collected. All samples were friable and weathered. Gleadow and Lovering's (1974) study showed that in the case of zircons, weathering has no effect on the retention of fission tracks.

Samples were eluted in seawater and initial separations were done using Harrison's panning technique. Heavy mineral separates were examined to determine abundance and quality of zircon population. Observations indicated that a bimodal distribution of zircons exists: clear, euhedral grains and rounded, variably radiation damaged grains.

Sample Preparation at SUNY- Albany

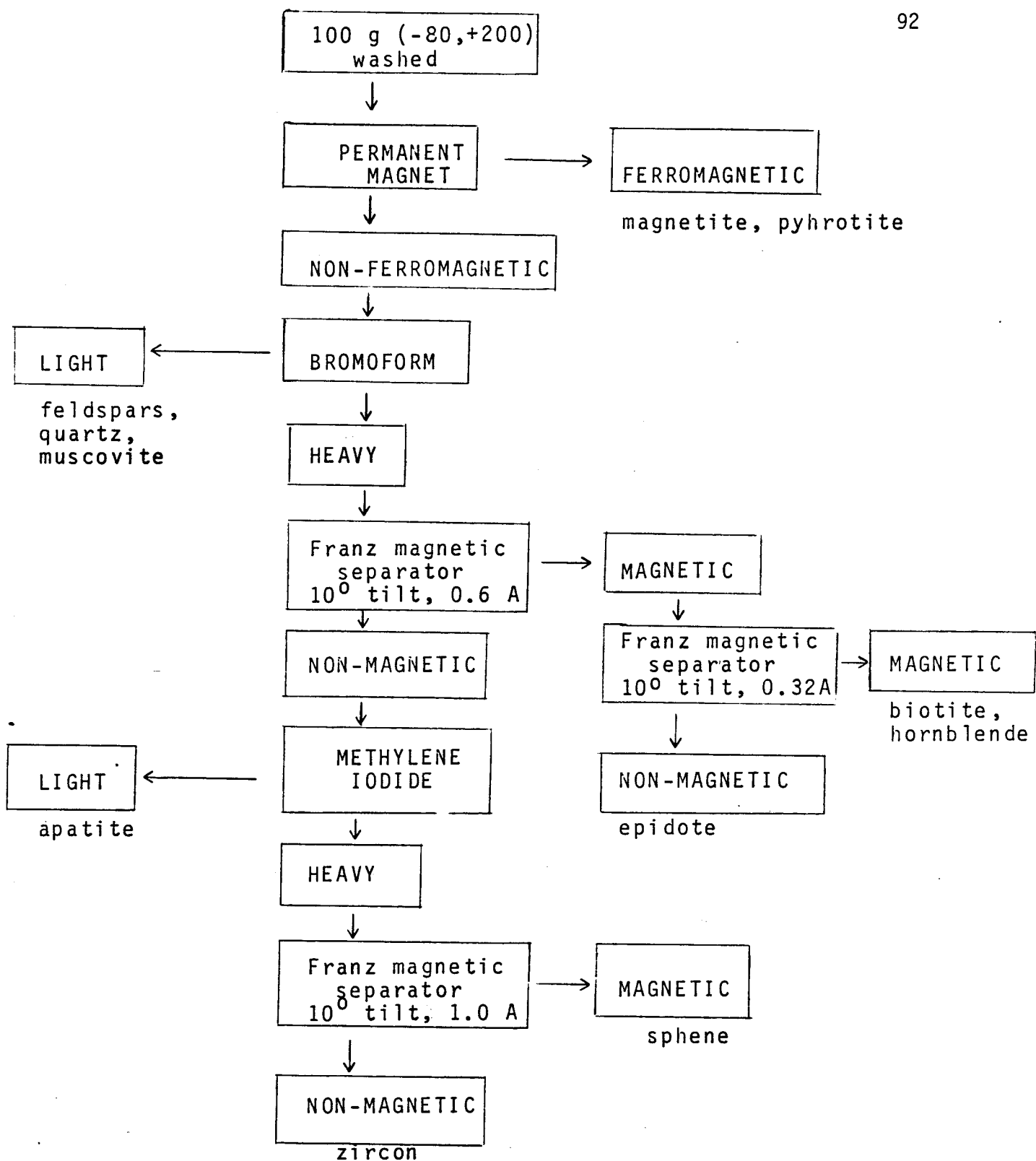
The following methods apply for sample preparations for zircons only. For preparation of apatite, sphene, etc. see Harrison (1979). Methods are summarized in the flow chart shown in figure 31.

Using sieves, the large grains can be removed. Samples can then be further separated using a Franz magnetic separator. Approximately 100 grams was placed in a separatory funnel containing bromoform (density approximately equal to 2.8 g/cm^3). (All heavy liquid separations should be done under a hood. Gloves and a lab coat should be worn.) After stirring the mixture well, the heavy minerals are allowed to settle to the bottom of the funnel (approximately 10 minutes). The material that settles to the bottom is drained into a funnel lined with filter paper. Light material will float to the top

of the funnel. All bromoform should be filtered back into a storage bottle. Next, one should wash both separates with acetone and place the filter paper containing heavy minerals onto a watch glass. Let these dry under heat lamps under a hood. Light minerals should be stored in labeled vials after they have dried completely (i.e. 12 hrs.). When the sample is completely dried, transfer the heavy minerals to the Franz magnetseparator. Set the Franz at 0.5 A on a 10 tilt. Pour the heavy minerals into a funnel and collect the nonmagnetic split. The magnetic minerals should be stored in a labeled vial. Non-magnetic separates are placed into separatory funnels containing methylene iodide, the material is stirred, and the heavy minerals are allowed to settle. Drain the heavy minerals into a filtered lined funnel in a beaker, wash with acetone, and transfer to clean filter paper. Wash with acetone again and dry the sample under heat lamps. The material remaining in the separatory funnel should be stirred well and let drain, with methylene iodide being saved in storage bottles. The residual should be washed with acetone twice and dried for 12 hrs. Store this separate in labelled vials. The heavy mineral separate is transferred to the Franz (10 tilt, 1 amp). Remove the magnetic separate and sieve the non-magnetic separate using 100 and 325 mesh. The end result should be a relatively clean zircon separate.

Because preliminary observations indicated the presence of a bimodal distribution of zircons, two mounts were made for each sample. Mounts were etched for different time periods (2 hrs. and 10 hrs.) to insure that all populations could be dated.

Clean Up Procedure



Note: Back-tilt for Franz Isodynamic Magnetic Separator should be 20°.

Figure 31: Mineral separatory techniques

Clean all glassware with acetone and then soapy water. Let all filter paper and waste dry thoroughly before discarding. Keep all bottles containing heavy liquids capped and under the hood at all times. If heavy liquid gets on clothing or skin, wash with acetone, then soapy water. Read chemical precautions before using heavy liquids.

Mounting Zircons In Teflon

Cut out two round pieces of teflon, 2cm in diameter, to fit in irradiation tube. Place aluminum block on a hot plate and heat to 310°C. Place a clean glass slide on Al block and allow it to come to 310°C. Place approximately 100 grains on another glass slide in an area of approximately 1 cm² and place this on the aluminum block. Carefully place two teflon discs on top of the grains. Place the heated slide on top of the discs, and gently squeeze together with tweezers or roller, being careful not to break the slides. The teflon will begin to melt. Continue to press and roll until the teflon becomes clear. Remove the slides from the hot plate and let them cool to room temperature. Check to see that the zircons are embedded in the teflon by observing the mount with a reflecting microscope. Scribe the sample number on the back of the teflon.

Polishing

When polishing, keep in mind that one wants to expose a surface at least one track length from the outside of the crystal (i.e., internal surfaces should be exposed). Attach the teflon mounts to a glass slide with wax (zircons face up!). Place the slide in the slide holder and gently remove approximately 20 um of the zircon by abrading the disc on

320 grit paper. Rotate the disc through 90° and repeat this procedure. Start with number 320 silicon carbide abrasive paper, then use number 400 and 600. Clean with distilled water. Attach microcloth discs to clean glass plates and place a small amount of aluminum oxide (5 um grit) onto the plate. Add water until a slurry forms. Continue polishing the mounts (moving in a figure 8 pattern) until the scratches are removed or polished. Rinse in distilled water and polish using 1 um grit followed by 0.3 um grit. If too much force is used when polishing, the grains will fall out of the teflon. After each step, check to be sure that the grains are still embedded in the teflon. The idea is to remove 20 microns from the surface of the grain- this is not alot of material!

Etching

If grains are underetched the tracks will be too faint to count. If they are overetched the tracks may overlap (if the density is high) and will make counting difficult. To determine the proper etching time, etch a sample for 2 hr, check it under a microscope, then etch longer if necessary.

Place circular aluminum template on a hot plate and heat to 210°C . Put 11.2 grams of KOH and 8.0 grams of NaOH in a Pt crucible and place on the Al block. When the eutectic NaOH-KOH mixture has reached 210°C , place the sample, zircon side up, in the liquid. The sample will float to the top. Place a funnel on top of the block and insert a teflon stirring rod into the liquid so that the mount remains covered with etchant. It is very important to keep the eutectic mixture at 210°C while the sample is being etched. If the temperature reaches 220°C or

higher the zircons will begin to fall out of the teflon (and you'll have to start all over!) The hot plate should be set to 3.0. A thermometer should be placed periodically in the eutectic mixture to check the temperature.

Two etching times were chosen depending on the crystal characteristics. For each sample all "A" mounts were etched for 10 hrs. and all "B" mounts for 2 hrs. In addition to the samples, a mount of Fish Canyon zircon was prepared for irradiation.

Preparing For Irradiation

To prepare samples for irradiation, cut low U mica into small pieces that will cover grains on mount. Cut two right angle corners and two oblique corners on each piece of mica. The shape of the detector should be irregular as this will enable one to easily determine which side has the induced tracks on it when etching the detector. Clean mount with distilled water. Using a strip of scotch tape, take a piece of muscovite and peel off the top surface exposing a clean cleavage surface. Carefully place the mica, clean surface face down on top of mount. Cover with piece of scotch tape making sure mica is attached securely to the mount. Trim off excess tape around edges. Repeat the above procedure until all mounts are covered with clean mica sheets and tape. Now take a pin and poke 4-6 holes into each sample making sure to pierce both mica and teflon. These holes will aid in trying to locate grain and mirror image of grain in detector.

Standard glasses NBS962 (Carpenter and Reimer, 1974) were used to determine the flux. Clean and cover two glass standards with muscovite detectors as described above. Cover with piece of scotch tape insuring

that the mica is securely attached to the mount. Scribe "T" and "B" for top and bottom on each piece of mica. Place mounts in order, record order and irradiation number in lab book. Measure thickness of samples and record. Place glass standards "B" mica side up in bottom of irradiation tube. Place samples in order into the tube mica side up. Glass standard "T" is placed on top with mica side down. Add enough packing material so that when the top of the irradiation tube is screwed on there will be no gaps between samples and standards. Consult advisor concerning the proper dose to be used (in this case, $1 \times 10^{15} \text{ n/cm}^2$).

Post Irradiation Procedure

If using Denver's TRIGA facility, samples will not be returned until they are safe to handle. Samples should be checked for the level of radioactivity before they are handled.

Place paper towels on lab bench and wearing gloves, empty contents of irradiation tube onto paper towels.

Etching Detectors

1) Standard detectors : Scribe "T" and "B" on detectors, respectively. One at a time, place in teflon beaker track side up. Add 48% HF and etch for one hour, then place on hot plate to boil off excess HF. Take clean glass slide and scribe standard number and "T" on it. Place a small amount of epoxy on slide and put detector "T" track side up on slide. Repeat for "B" detector.

2) Samples: Remove mica detectors from samples one at a time and place in 48% HF in teflon cup under hood at 25°C . After eleven minutes add water to dilute HF, transfer to large beaker, and dilute again. Rinse

mica with ethanol and distilled water and place on slide. Place slide on aluminum block on hot plate at 125°C to boil off excess HF. The mica will fizz and/or etch the glass. Place two drops of epoxy on glass slide that has been scribed with sample number. Place teflon mount and mica detector side by side on glass slide making sure that both have track sides facing up!

Counting Fission Tracks

Fission tracks must be straight, randomly oriented, and 10-20 micrometers in length. It is easy to distinguish fission tracks from dislocations because dislocations often have curved etch pits, have preferred orientation, occur in swarms, and may be longer than fission tracks.

Spontaneous and induced tracks must be counted on the same area on the grain. Use an oil emersion lens at 1250x when counting tracks. It is necessary to calibrate grid using a micrometer before counting tracks.

Flux Determination

Count induced tracks in 500 random areas in each standard detector at 500x. Multiply induced track density by calibration factor (4.94 x 10⁻⁹) (Harrison, per. comm.) to determine flux. Repeat this procedure for top and bottom detectors. Plot flux vs. distance (bottom detector at 0.0 cm) for detectors. Assume a linear relationship between flux and distance to determine the neutron dose for each sample. Fish Canyon zircon can be used as an internal check on the flux determination.